IXPE
Imaging
X-Ray
Polarimetry
Explorer

Marshall Space Flight Center

agenzia spaziale italiana

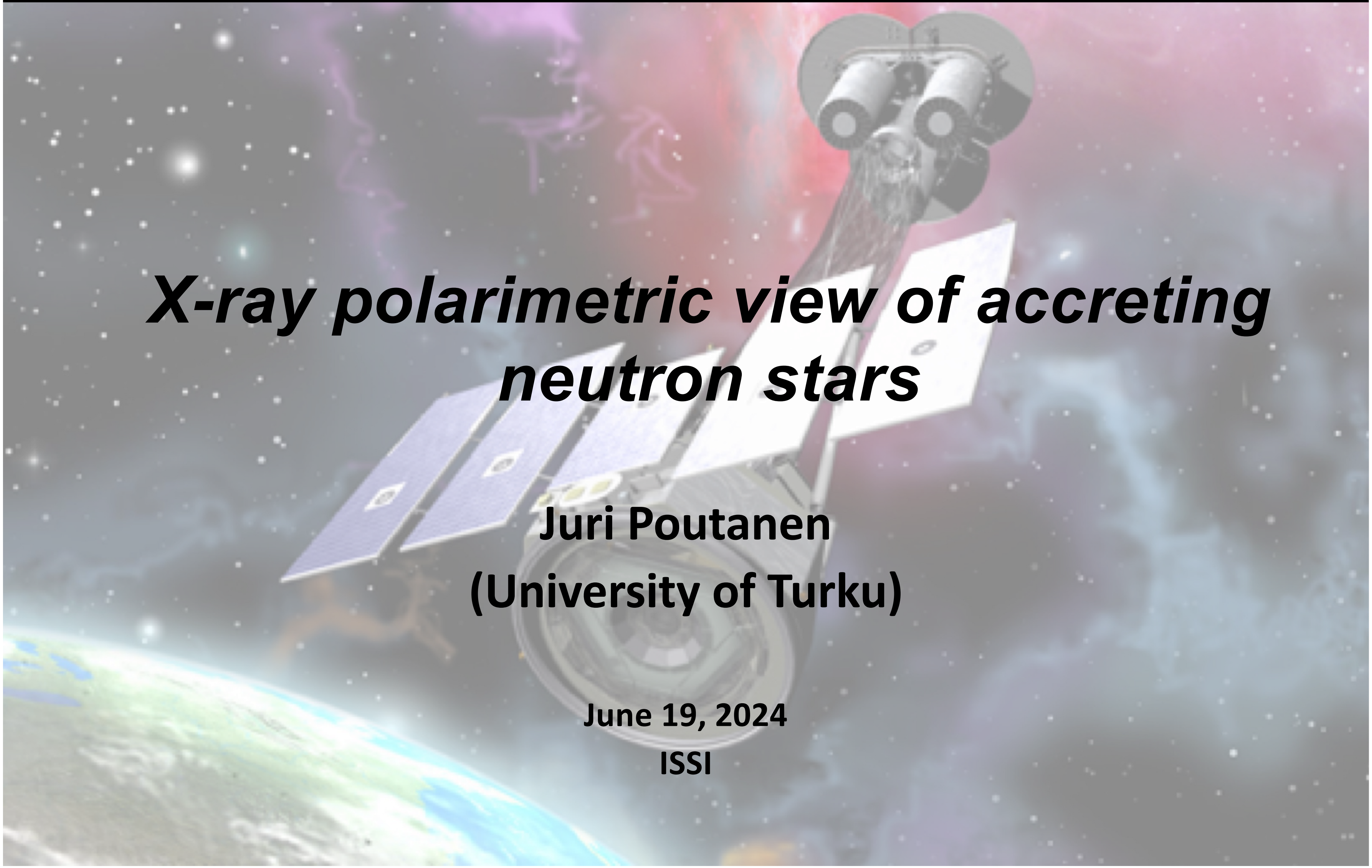

X-ray polarimetric view of accreting neutron stars

Juri Poutanen

(University of Turku)

June 19, 2024

ISSI

IXPE
Imaging X-Ray Polarimetry Explorer

X-ray pulsars

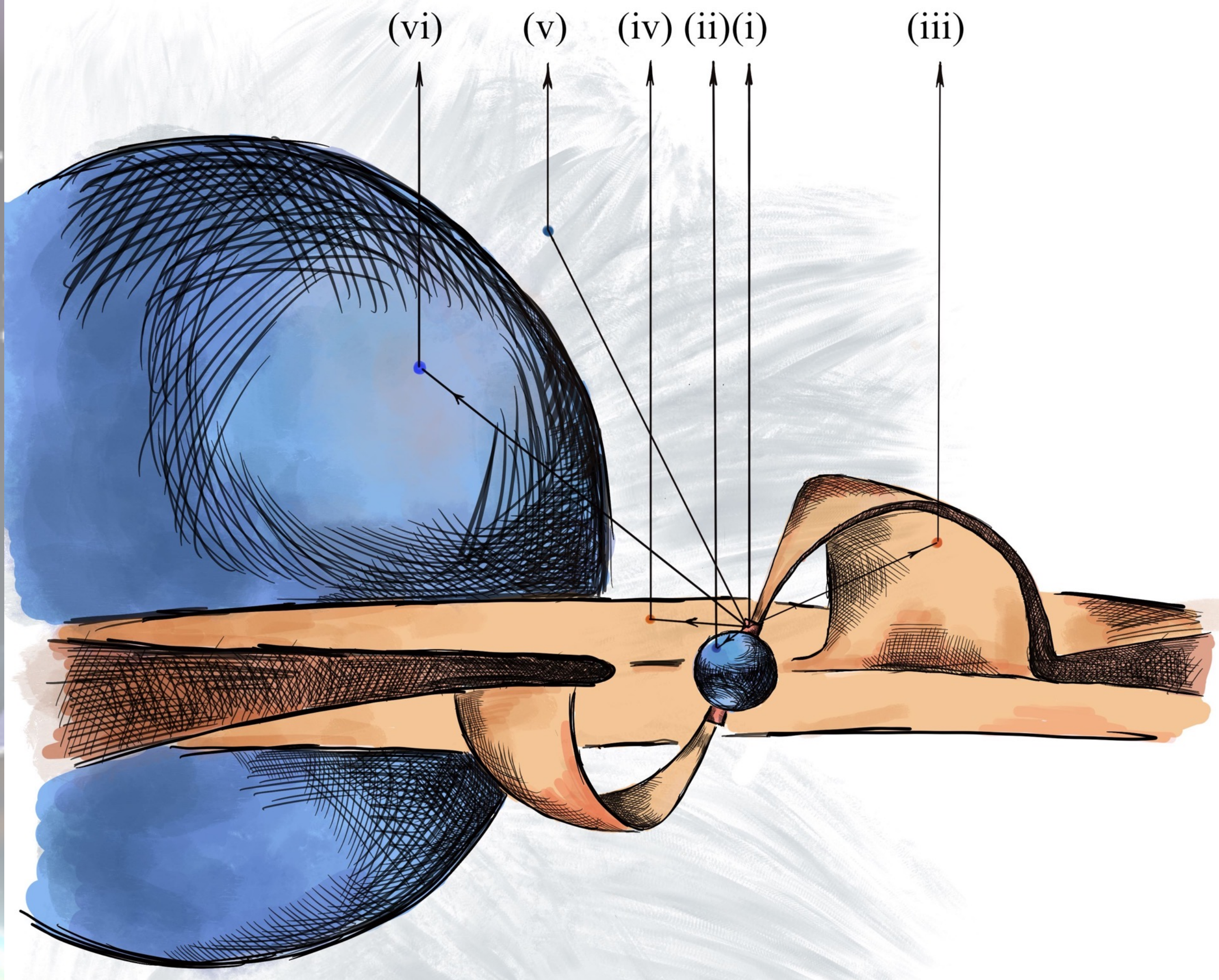

X-ray pulsars

Main goals

- Determining geometry of the emitting region (hotspot vs column) and emission pattern (fan vs pencil beam) at different luminosity levels

- Revealing evidence for non-dipolar fields

- Test free-precession model for Her X-1

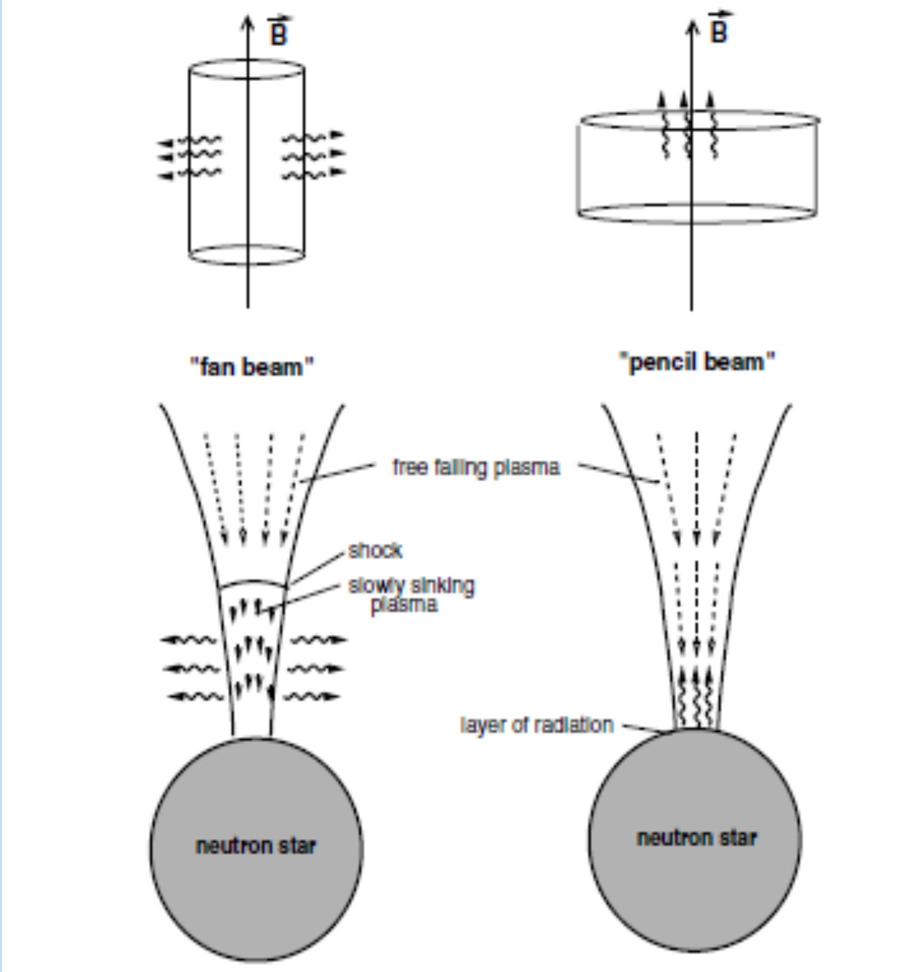

Meszaros et al. 1988

X-ray pulsars

Opacity in highly magnetized plasma:

$k_{\perp} \approx (E/E_B)^2\, k_{\parallel}$ $E<E_B = 11.6\ (B_{12})$ keV

(electron cyclotron energy)

where $k_{\perp}$ and ($k_{\parallel}$) are the opacities in the Extraordinary (Ordinary) modes, when the wave electron field is perpendicular (parallel) to the plane defined by the line of propagation and the external magnetic field

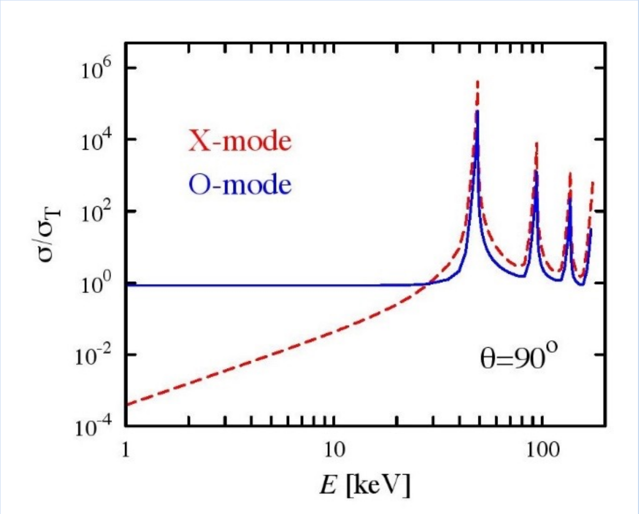

Mushtukov et al. 2016

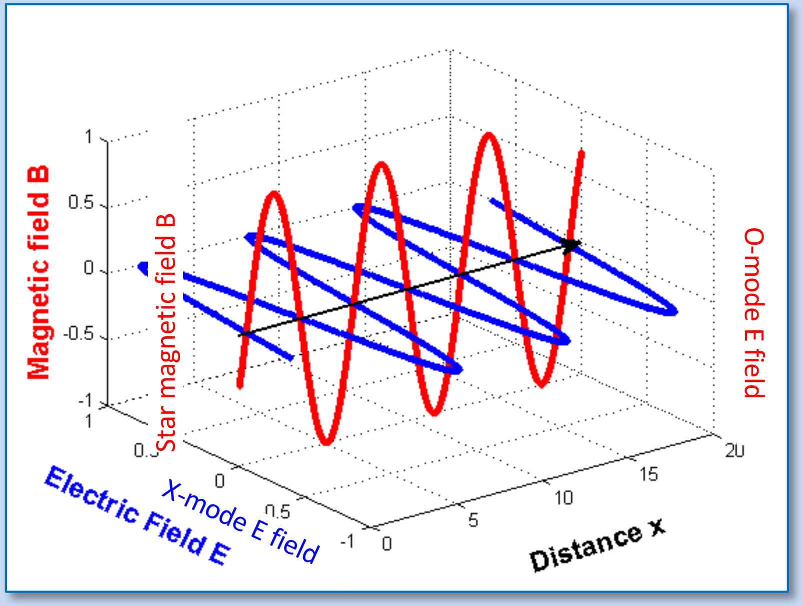

O-mode: the **E**-field oscillates in the **k-B** plane

X-mode: the **E**-field oscillates ⊥ to the **k-B** plane

Rotating Vector Model (RVM)

- Magnetic dipole misaligned from the rotation axis.
- Pulse phase dependence of the polarization angle (position angle of the dipole) .
- Rotating vector model of Radhakrishnan & Cooke (1969), Meszaros et al. (1988)

$$\tan(\chi - \chi_p) = \frac{-\sin\theta_p \sin\phi}{\sin i_p \cos\theta_p - \cos i_p \sin\theta_p \cos\phi}$$

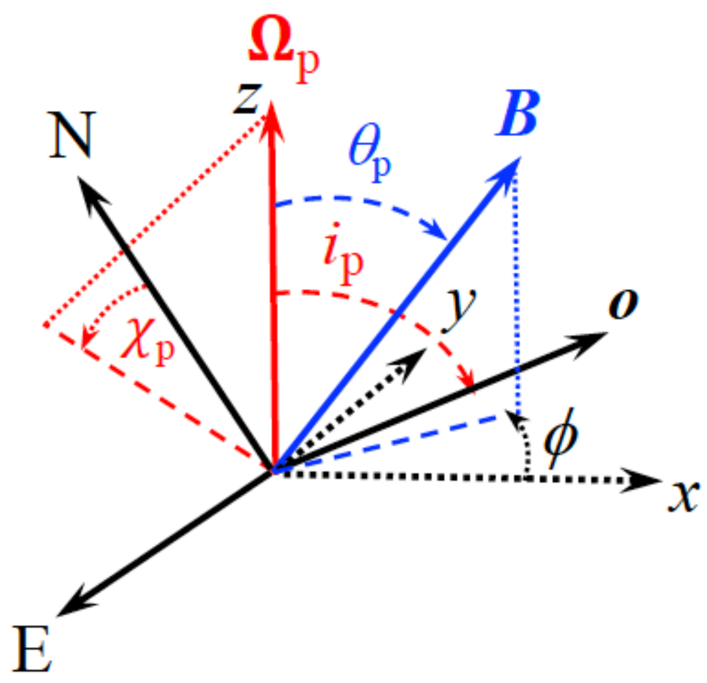

χ_p - position angle of the pulsar spin

i_p - observer inclination relative to the pulsar spin

θ_p - magnetic obliquity

ϕ - pulsar phase

https://www.youtube.com/watch?v=mXzwtp-KaoI

IXPE
Imaging X-Ray Polarimetry Explorer

RVM: examples

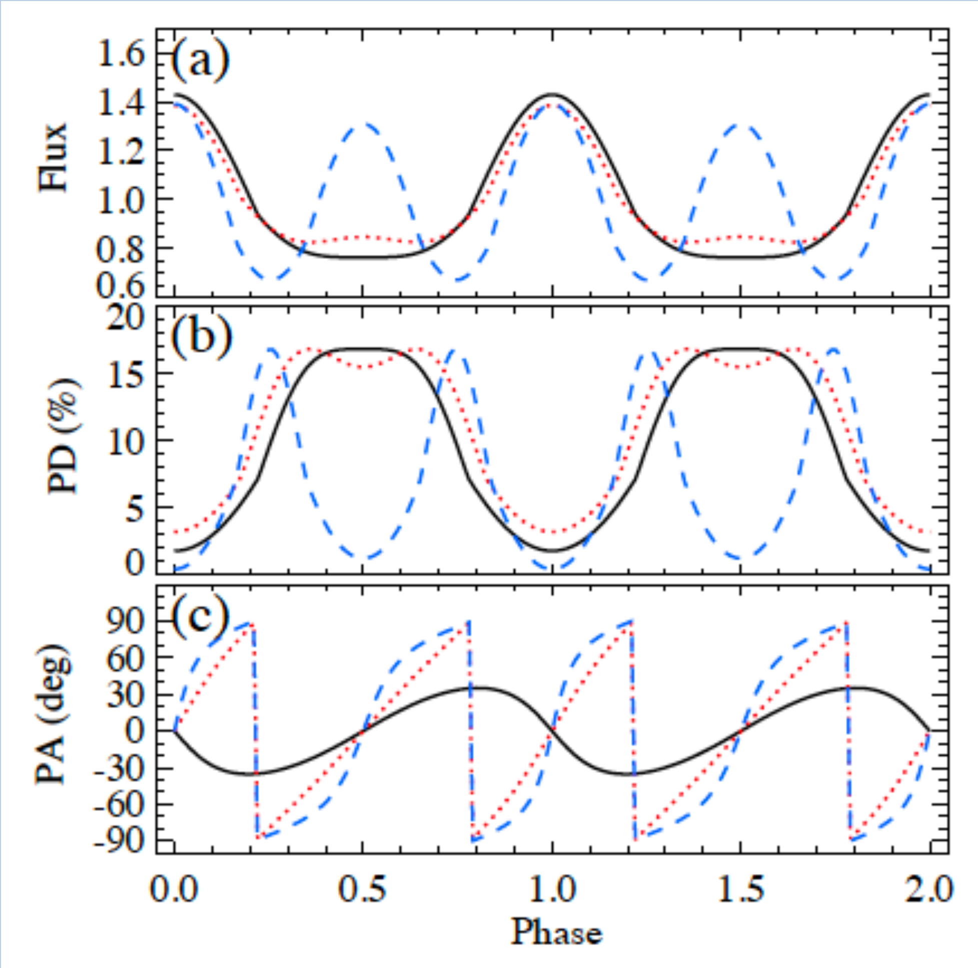

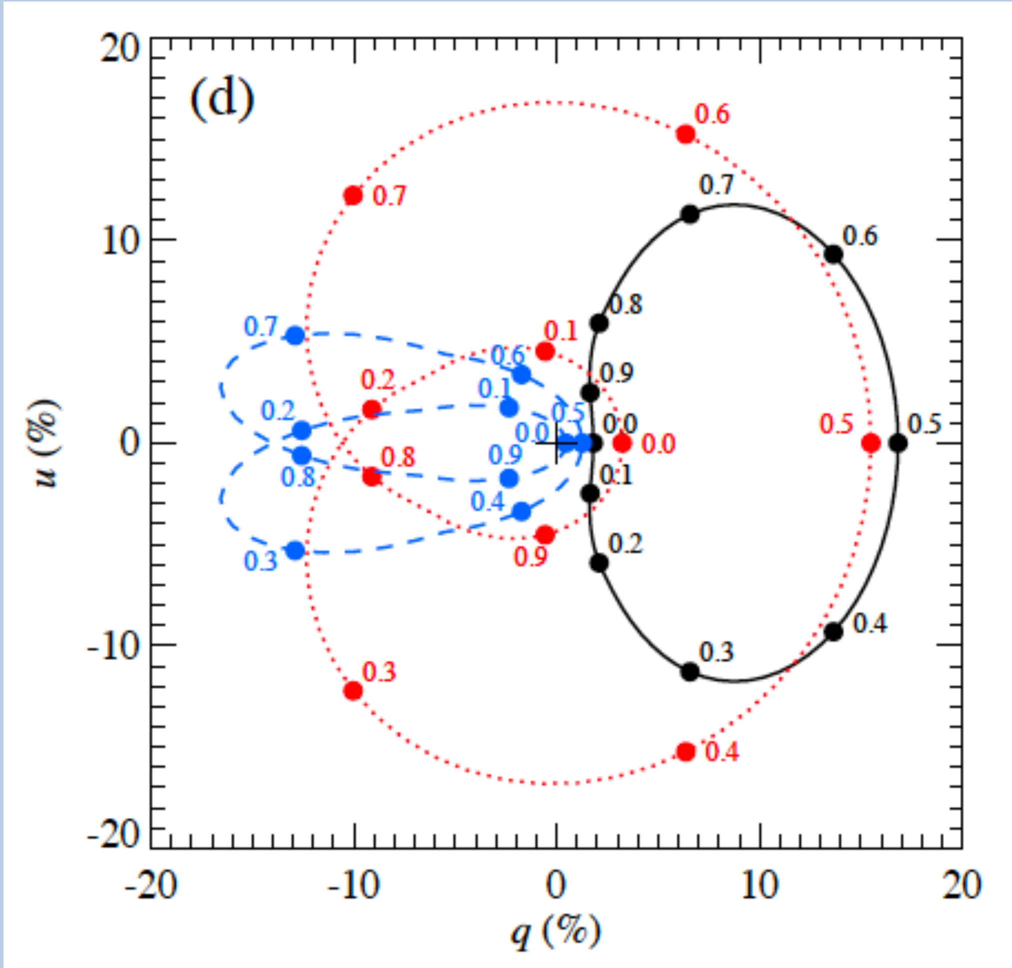

$(i_p, \theta_p)=(60°, 30°)$
black

$(30°, 70°)$
red

$(70°, 85°)$
blue

IXPE
Imaging
X-Ray
Polarimetry
Explorer

IXPE: X-ray pulsars

Name	Spin Period[a,b] [s]	Orbital Period[a,b] [d]	Distance[a,b] [kpc]	Luminosity[c] [erg s^{-1}]	CRSF [d] [keV]
Cen X-3	4.8	2.09	6.07	1.9×10^{37}	28
Her X-1	1.24	1.7	7.09	$\sim 3 \times 10^{37}$	37
4U 1626−67	7.7	0.02875	15.08	6.4×10^{36}	37, 61?
Vela X-1	283	8.96	1.87	3.8×10^{35}	25, 53
GRO J1008−57	93.5	249.5	3.21	$(0.6 - 1.6) \times 10^{36}$	78
EXO 2030+375	41.31	46.02	2.08	1.3×10^{36}	36/63?
X Persei	837.67	250.3	0.63	1.2×10^{34}	29
GX 301−2	696.0	41.59	3.54	1.3×10^{36}	37/50
LS V +44 17	202.5	155.0	2.29	$\leq 4 \times 10^{37}$	32
Swift J0243.6+6124	9.87	28.3	5.2	$(0.6 - 2.4) \times 10^{37}$	146
SMC X-1	0.717	3.892	61	2×10^{38}	–

IXPE: X-ray pulsars

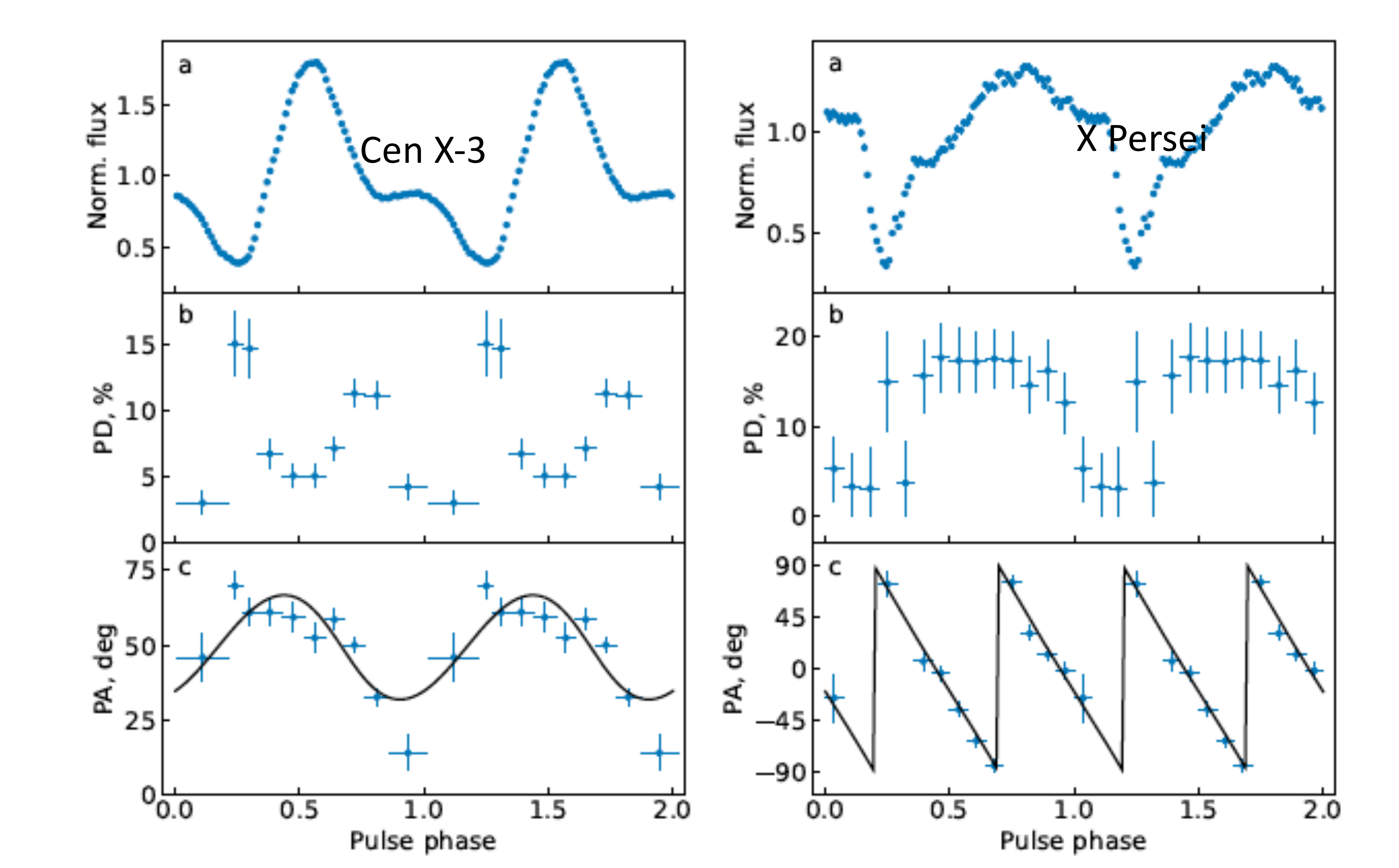

- **Well fitted by the RVM**

IXPE: X-ray pulsars

IXPE
Imaging X-Ray Polarimetry Explorer

Cen X-3

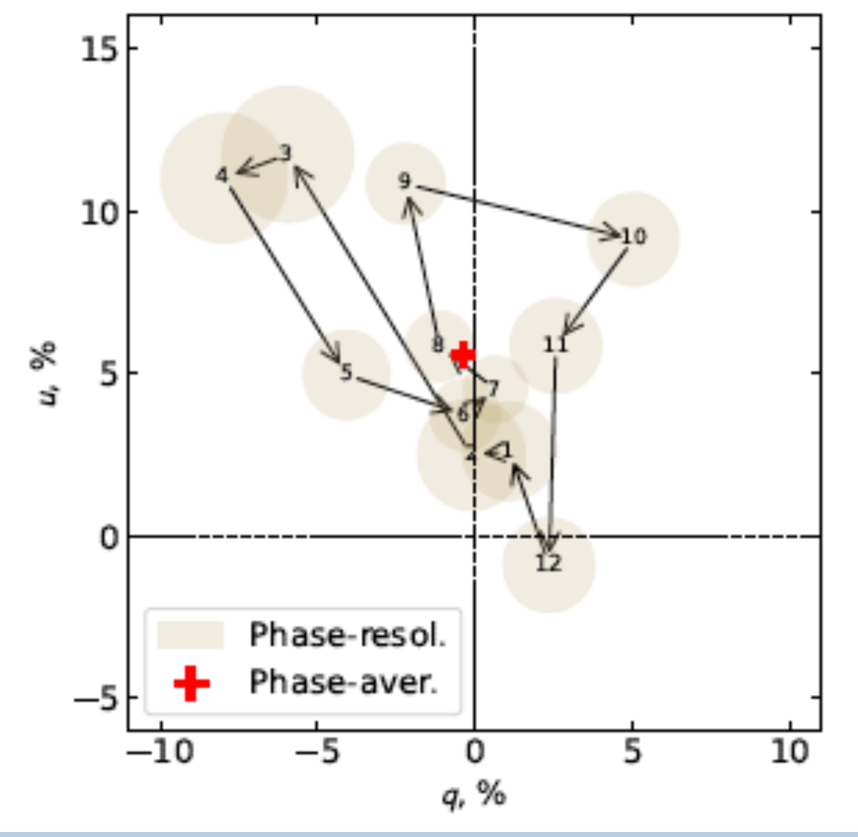

X Persei

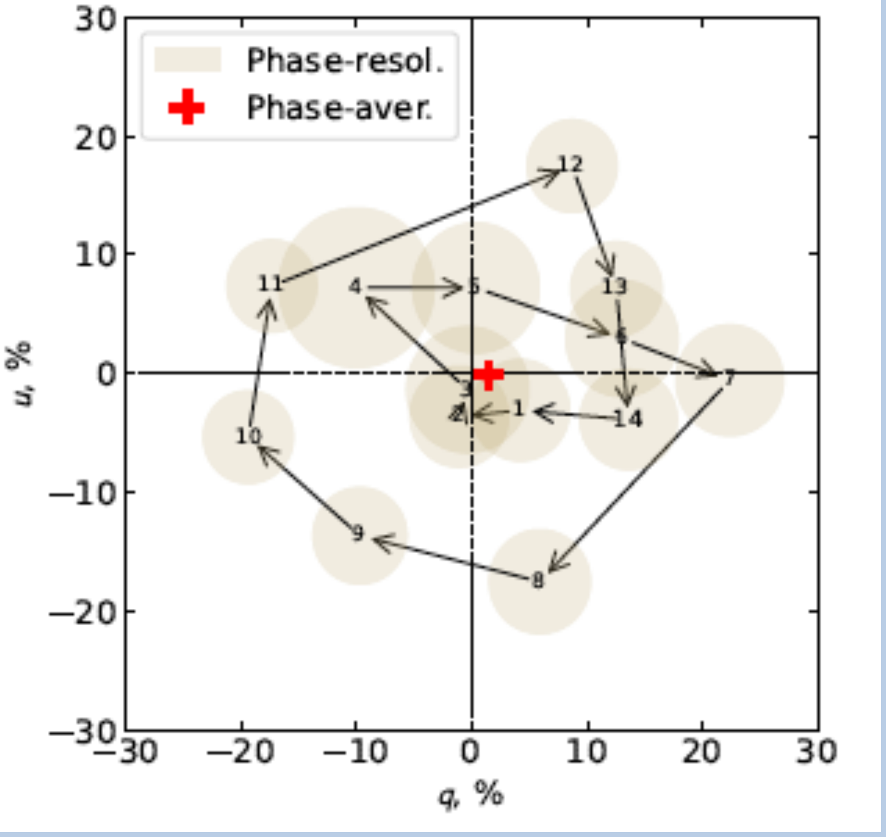

The case of Her X-1

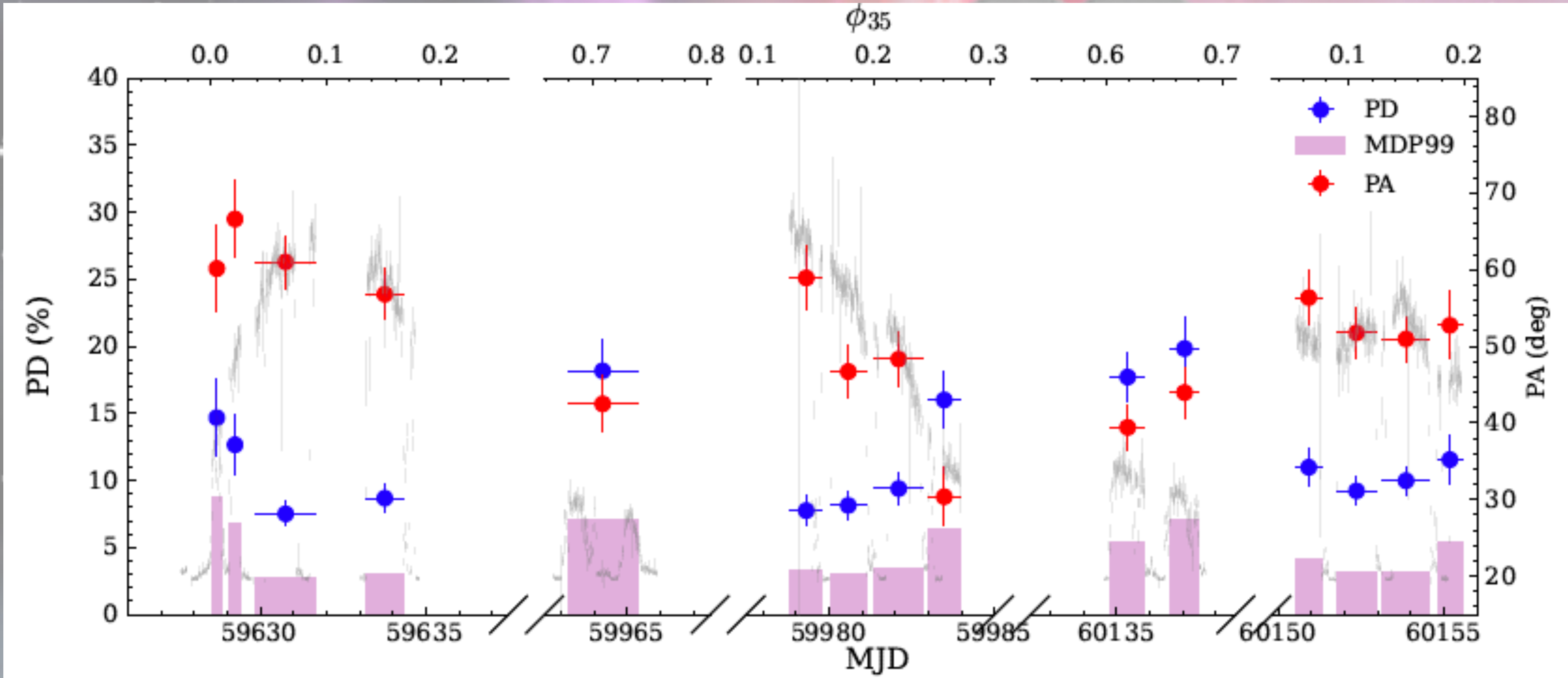

- Observed three times in the so-called “main on” or “high on” state and two times in the ”short-on”.

Doroshenko+ 2022, Nat Astro; Heyl+ 2024, Nat Astro; Zhao+ 2024, MNRAS

Time dependence of X-ray polarization

IXPE
Imaging X-Ray Polarimetry Explorer

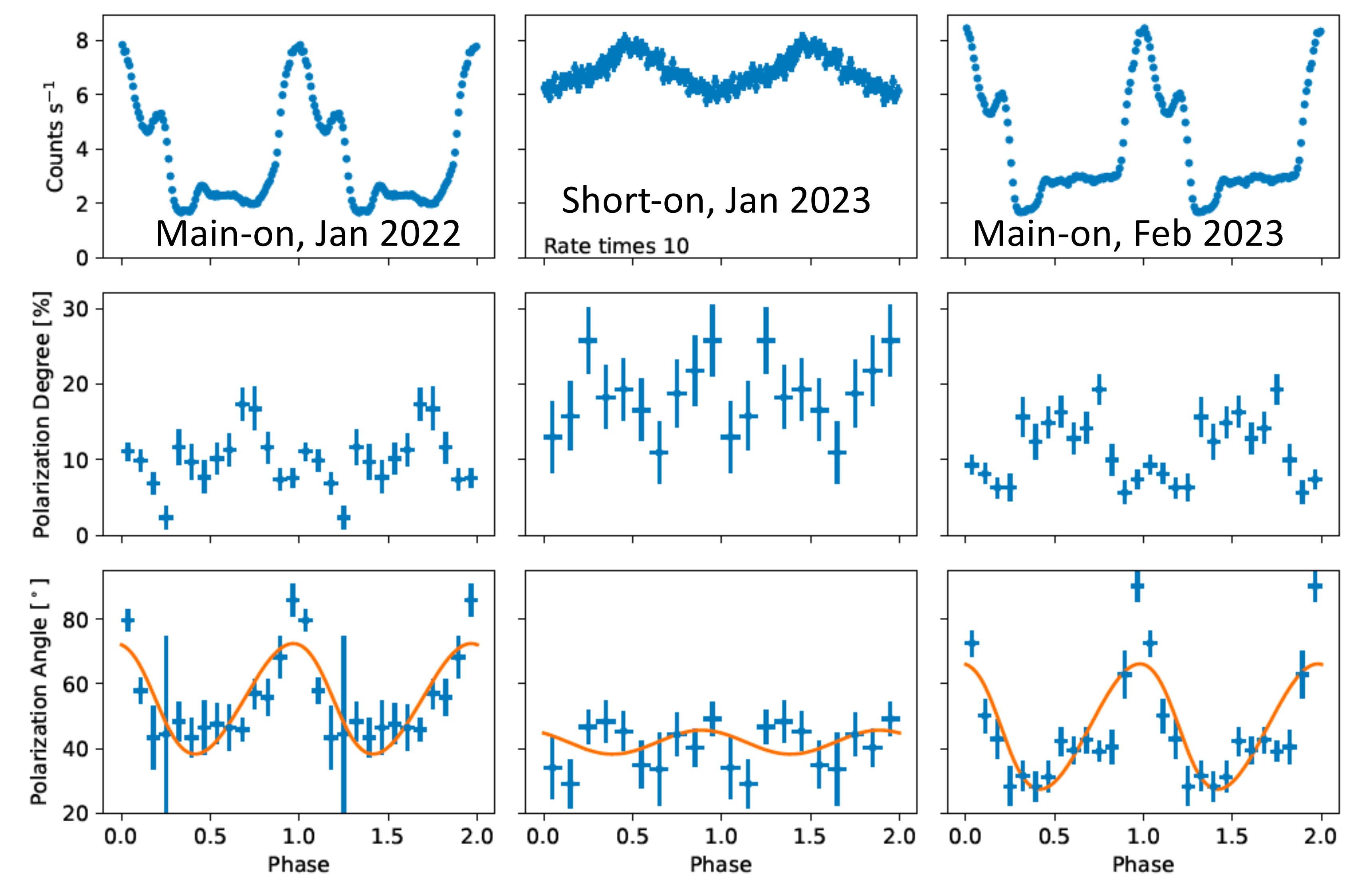

Doroshenko+ 2022, Nat Astro; Heyl+ 2024, Nat Astro; Zhao+ 2024, MNRAS

Time dependence of X-ray polarization

	Mean PD (%)	i_p (deg)	θ (deg)	χ_p (deg)	ϕ_0 (%)	Prec. Phase (%)
First Main-On	9.5 ± 0.5	58^{+28}_{-22}	$14.5^{+3.0}_{-4.0}$	55.4 ± 1.6	$19.0^{+2.7}_{-2.2}$	8.8
Early	8.6 ± 0.6	64^{+25}_{-22}	$16.3^{+3.5}_{-4.1}$	57.9 ± 2.1	$19.0^{+2.6}_{-2.4}$	7.3
Late	9.3 ± 0.7	85^{+35}_{-37}	$15.9^{+3.6}_{-4.0}$	52.2 ± 2.7	$21.7^{+4.5}_{-5.0}$	16.2
Short-On	17.8 ± 1.4	90^{+30}_{-30}	$3.7^{+2.6}_{-1.9}$	41.9 ± 2.2	85.1^{+18}_{-19}	68.7
Second Main-On	9.1 ± 0.5	56^{+24}_{-20}	$16.0^{+3.1}_{-4.3}$	46.8 ± 1.5	$19.8^{+2.3}_{-2.0}$	15.9

Heyl et al. 2024

Strong indication of precession!

Requires deviations from sphericity at 10^{-7} level

Time dependence of X-ray polarization

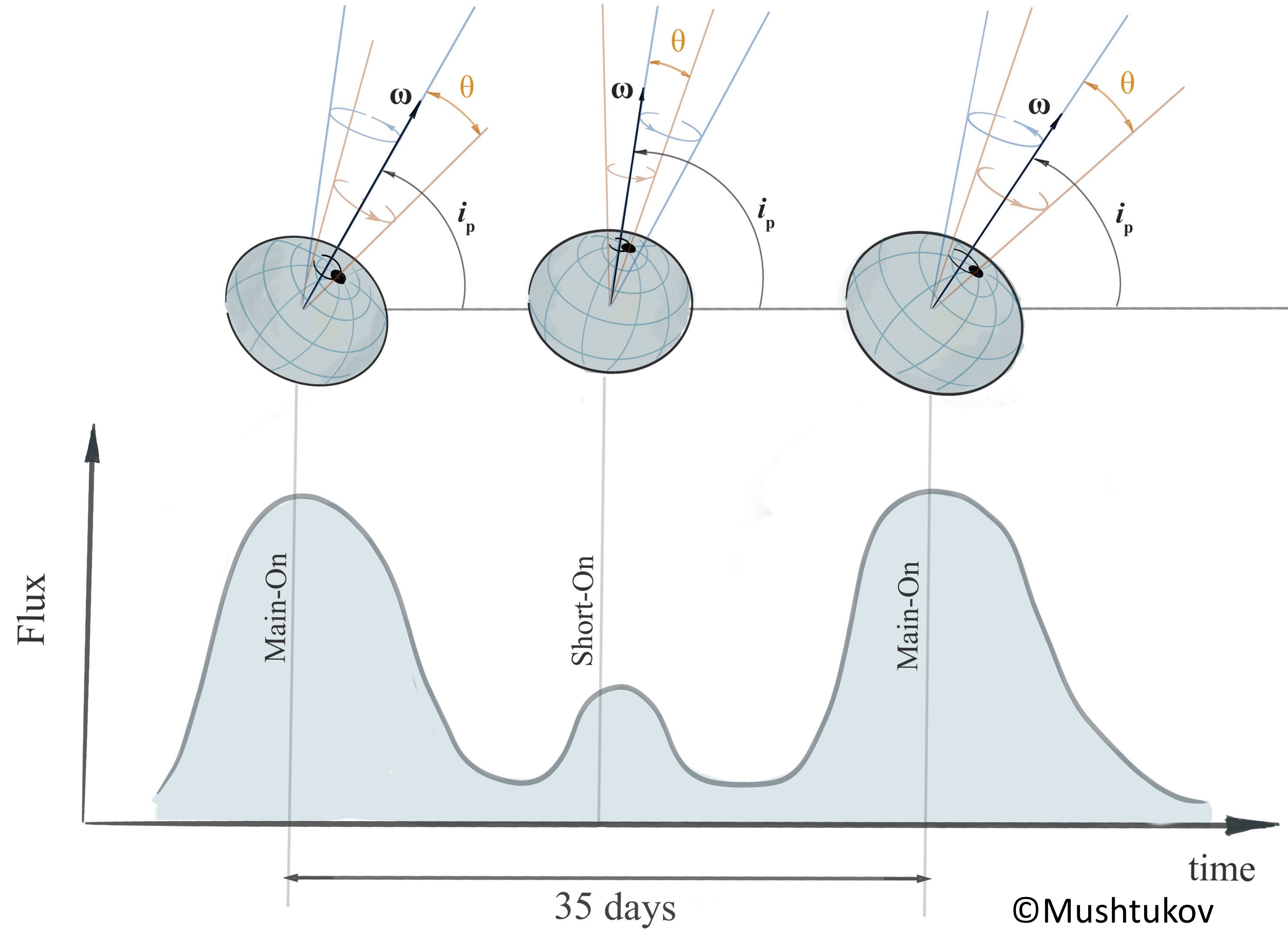

Giant outburst of LS V +44 17 / RX J0440.9+4431

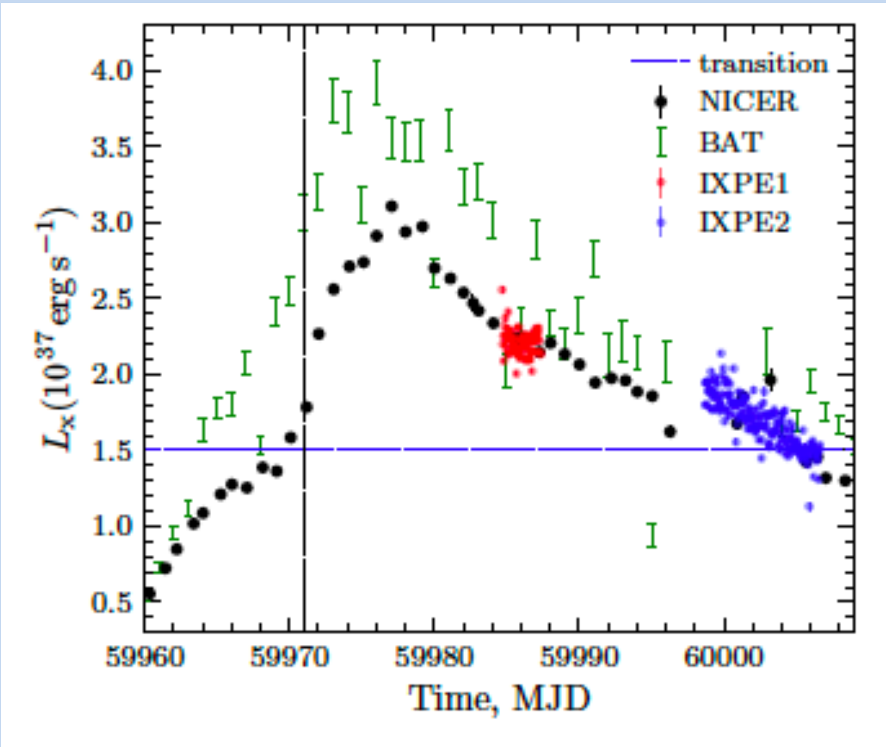

Doroshenko et al. 2023

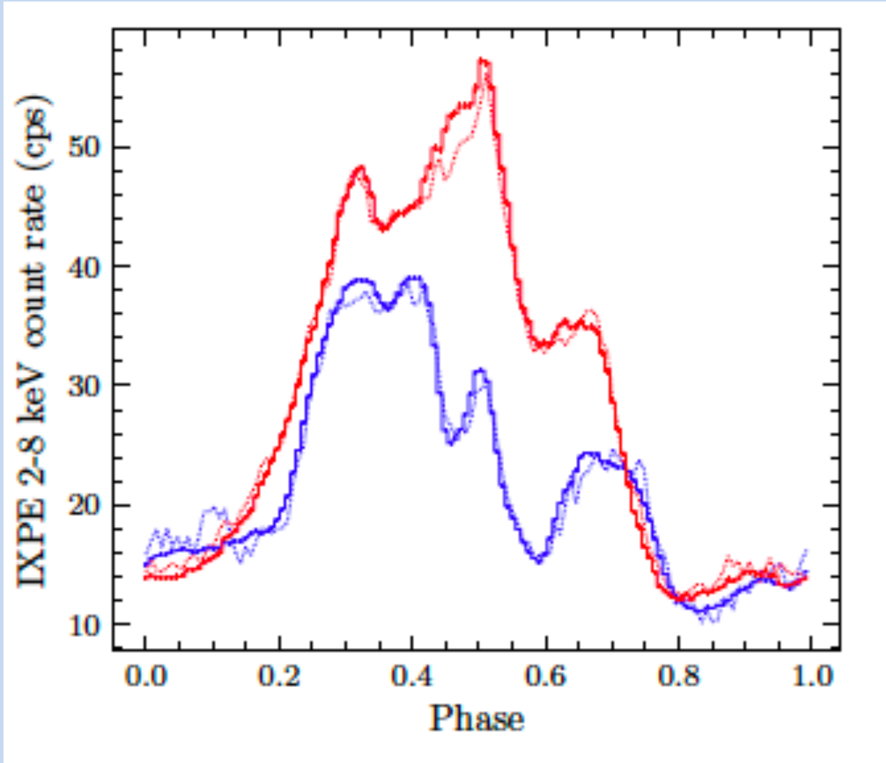

NICER and IXPE pulse profiles

IXPE
Imaging X-Ray Polarimetry Explorer

Phase-resolved polarimetry

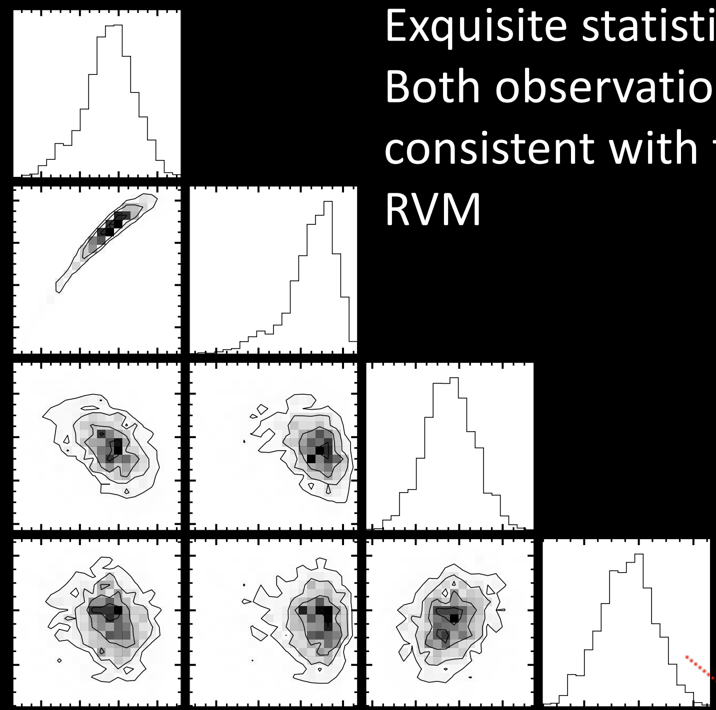

Exquisite statistics- Both observations consistent with the RVM

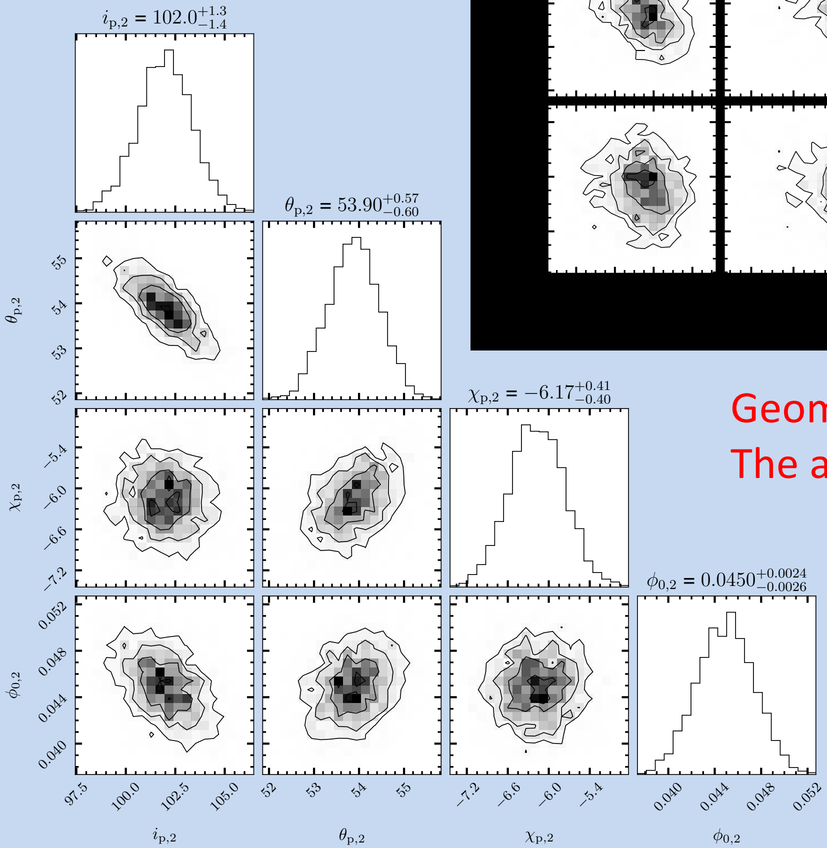

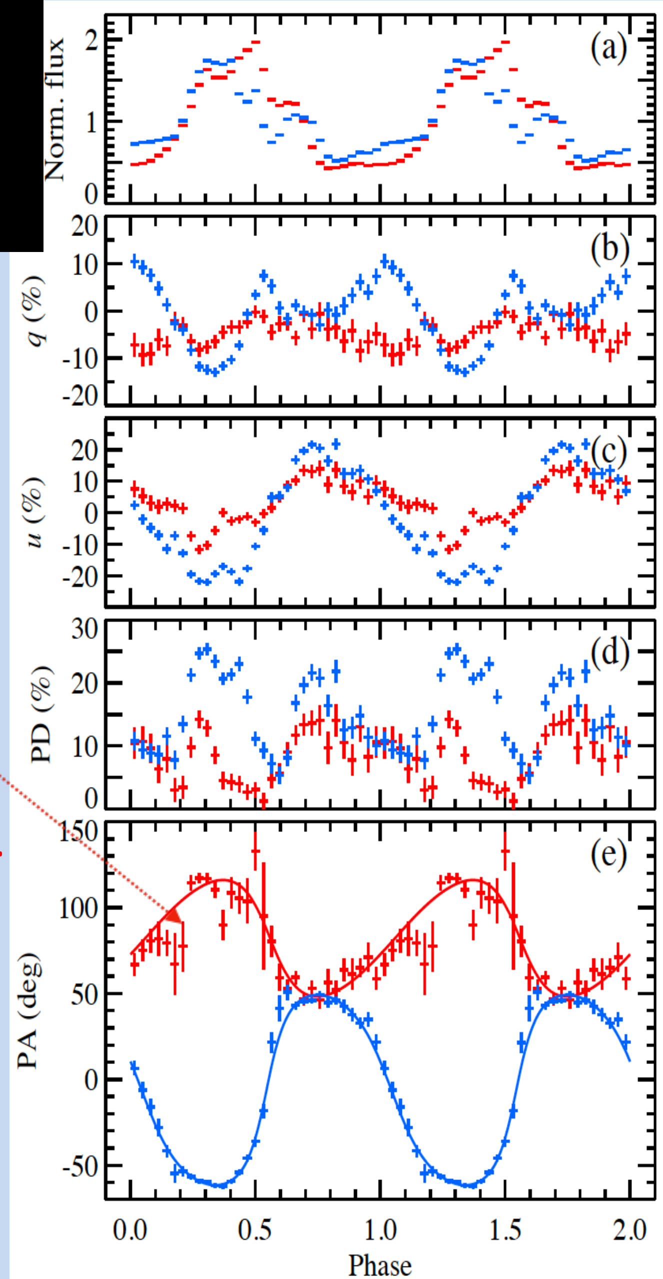

Geometry is dramatically different. The angles changed by

$$\Delta i_p \sim 46^\circ$$

$$\Delta \theta_p \sim 30^\circ$$

$$\Delta \chi_p \sim 90^\circ$$

$$\Delta \phi_0 \sim 0.5$$

...in 10 days

Two-component polarization model

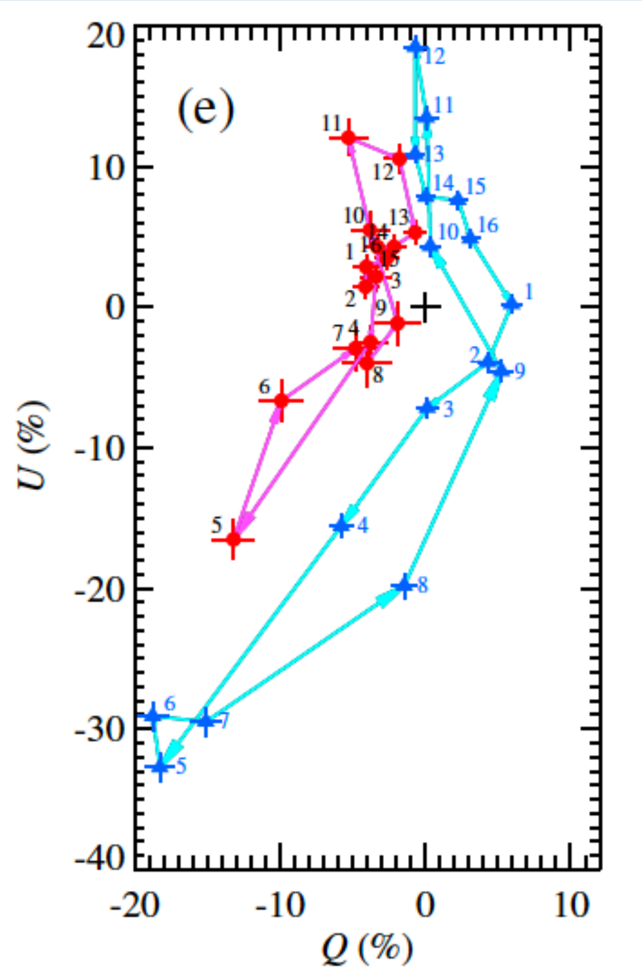

Work in Q/U space

$$
\begin{aligned}
I(\phi) &= I_c + I_p(\phi), \\
Q(\phi) &= Q_c + P_p(\phi) I_p(\phi) \cos[2\chi(\phi)], \\
U(\phi) &= U_c + P_p(\phi) I_p(\phi) \sin[2\chi(\phi)].
\end{aligned}
$$

observed constant RVM-part

$$
\tan(\chi - \chi_p) = \frac{-\sin\theta \ \sin[2\pi(\phi - \phi_0)]}{\sin i_p \cos\theta - \cos i_p \sin\theta \cos[2\pi(\phi - \phi_0)]}
$$

- Assume constant + RVM components
- RVM parameters constrained through comparison with observed Q/U
- **Only the product $P_c I_c$ is constrained, not flux or P individually** *(can have low-intensity strongly polarised background or high-intensity weakly polarised background)*

Marshall Space Flight Center

agenzia spaziale italiana

IXPE
Imaging
X-Ray
Polarimetry
Explorer

Two-component polarization model

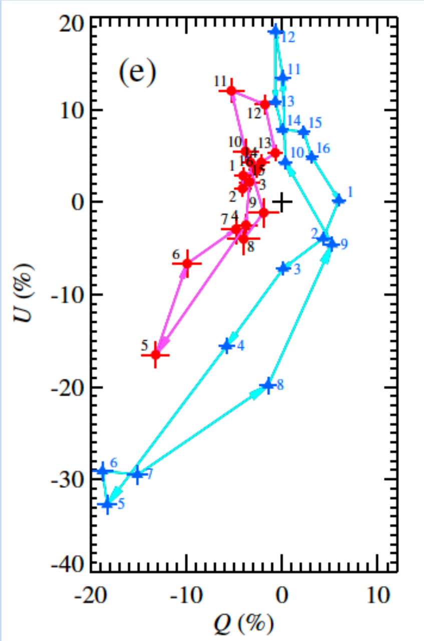

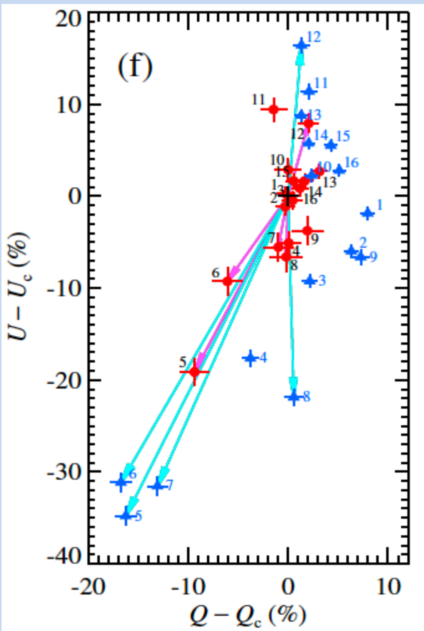

Original (Q, U)=(q,u)*F*/⟨*F*⟩ and PA

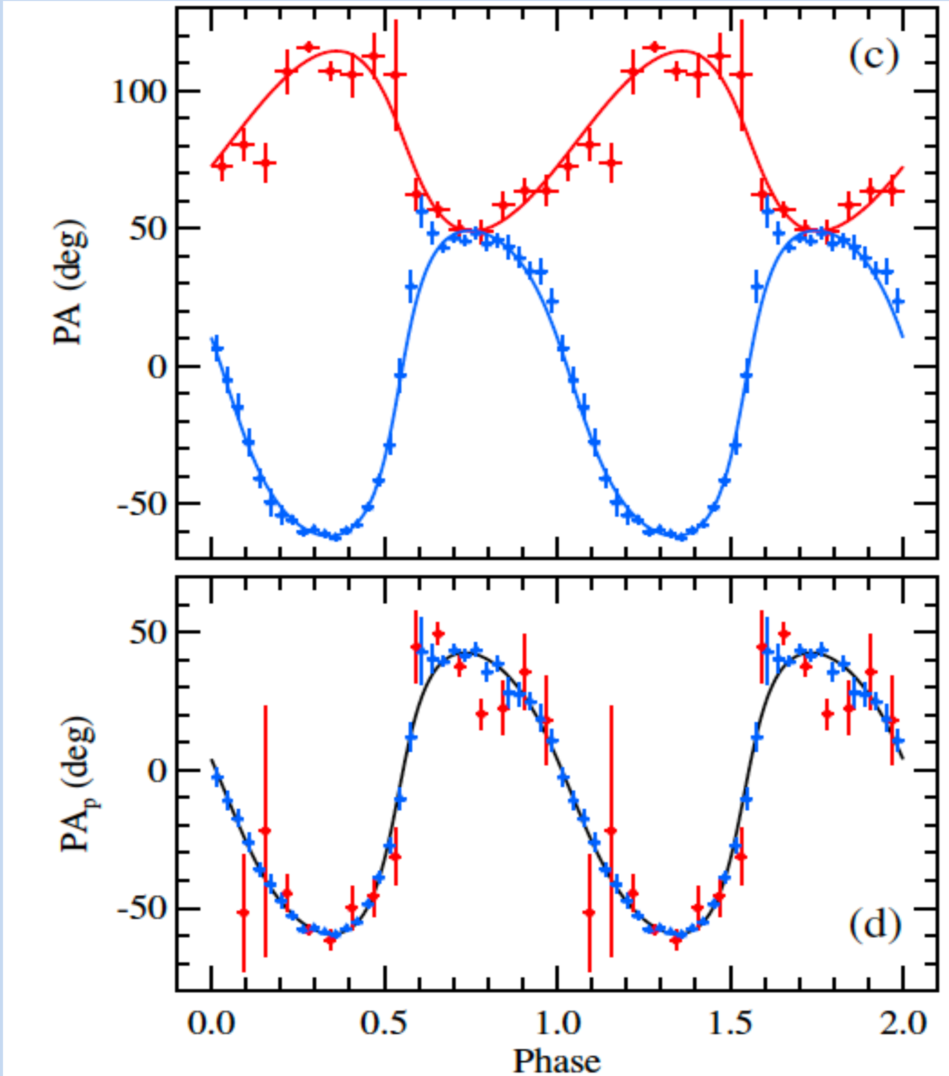

Corrected (Q-Q_c, U-U_c) and PA

$$P_{c,i} I_{c,i} = \sqrt{Q_{c,i}^2 + U_{c,i}^2}$$

4.5% ± 0.3% and 2.9% ± 0.4%

$$\chi_{c,1} = 72^\circ \pm 2^\circ \text{ and } \chi_{c,2} = 67^\circ \pm 4^\circ$$

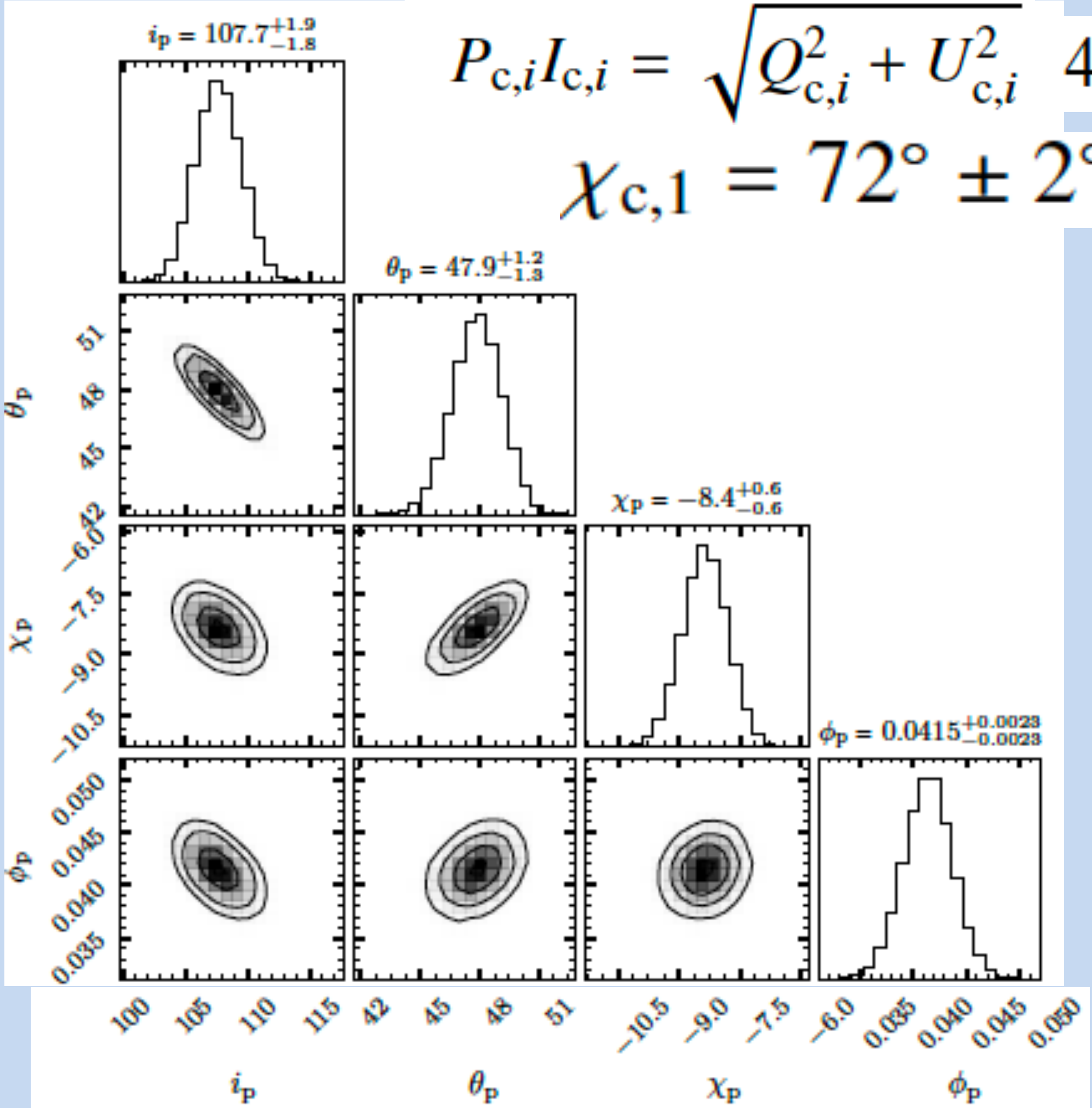

Doroshenko et al. 2023

Origin of the unpulsed component

- What is it? It should be, e.g., 20% polarized and give 20% of observed flux?

Unpulsed = relatively far away from NS: scattering in disk/disk wind?

- **PD up to ~33%** due to scattering in equatorial wind (Sunyaev & Titarchuk 1985)

- There is evidence for presence of strong outflows in BeXRBs from radio and X-ray data with **up to 20% flux in reflected/scattered component** (although at higher L_x).

- LS V +44 17 is viewed **~edge-on**, polarization due to scattering is expected to be high (Nitindala et al.)

- PA of constant component be aligned with optical polarization (Be-disk is expected to be aligned with the accretion disk) which seems to be indeed the case. We get **PA~72(2)° and 67(4)°** for the first and 2nd observation, optical polarimetry gives **60-70° in BVR** (Nitindala et al. 2023)

Non-magnetic accreting neutron stars

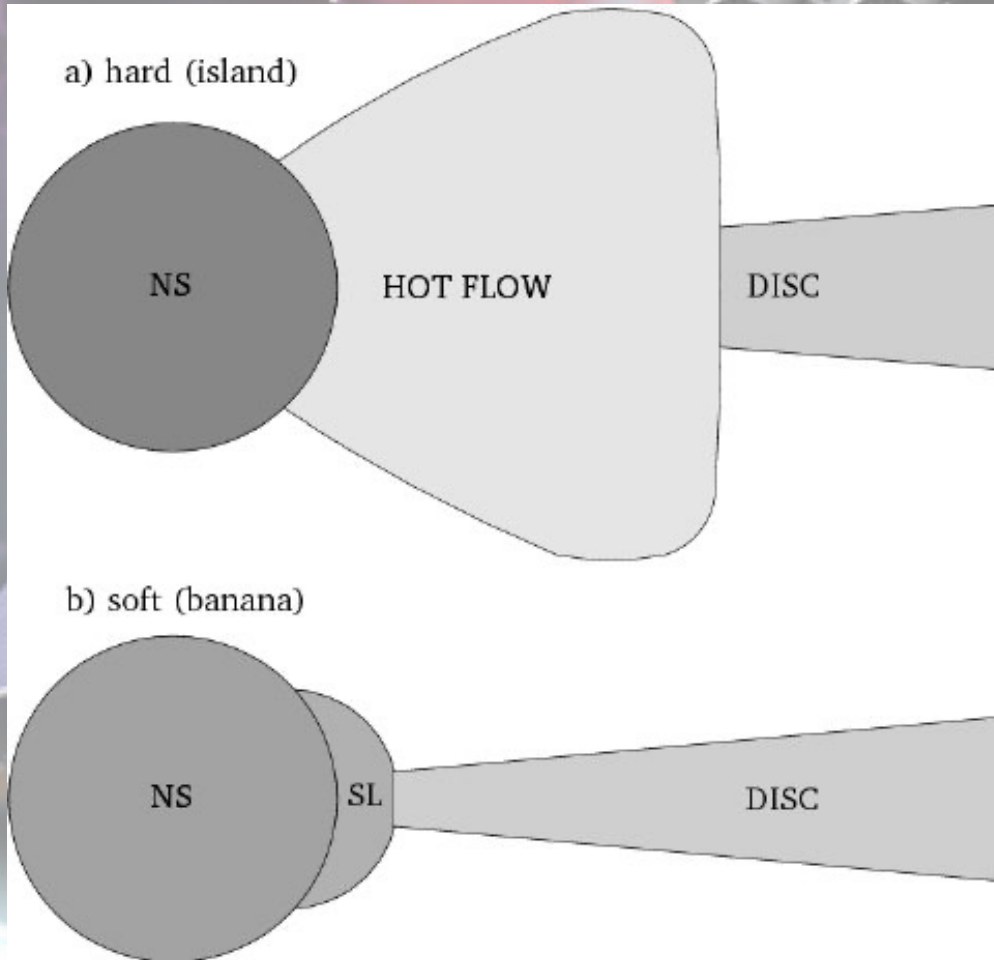

Nonmagnetic NS

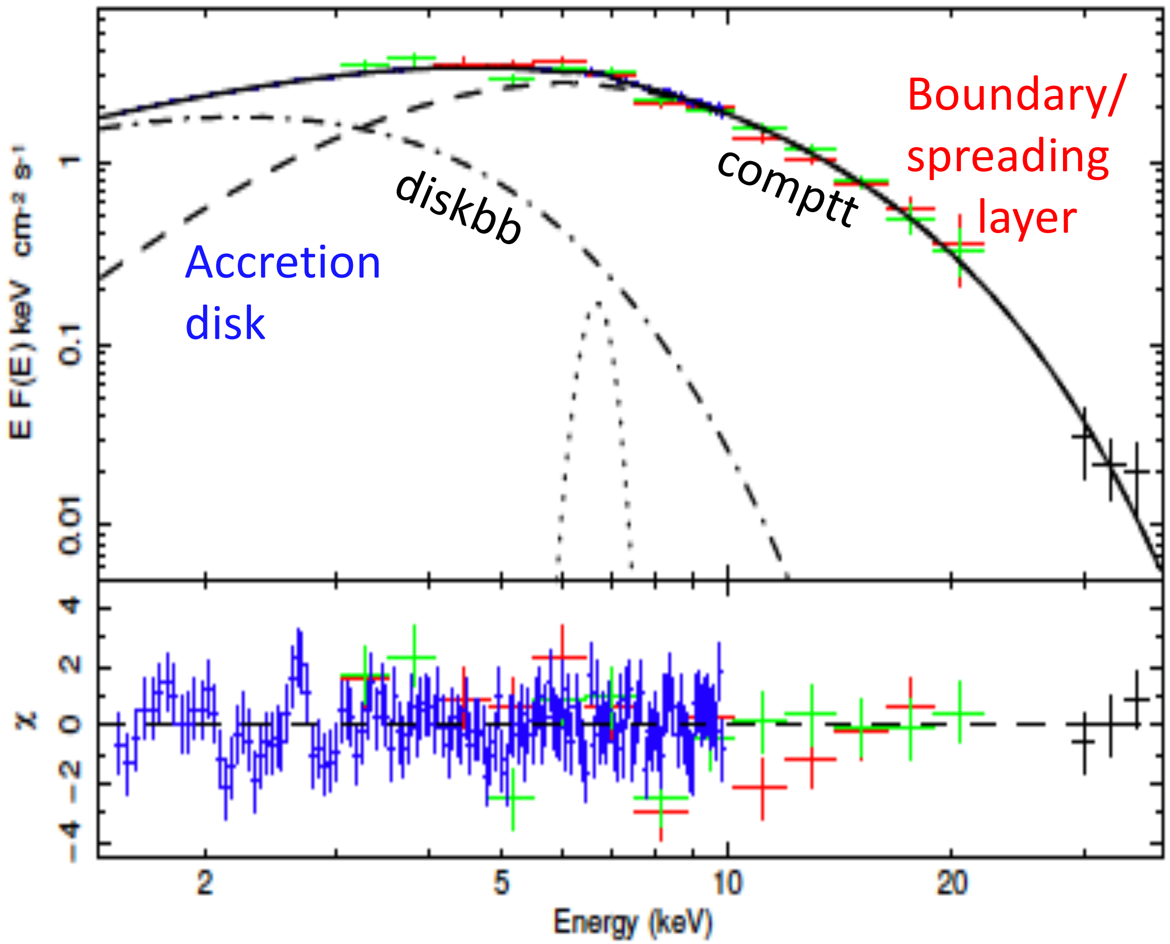

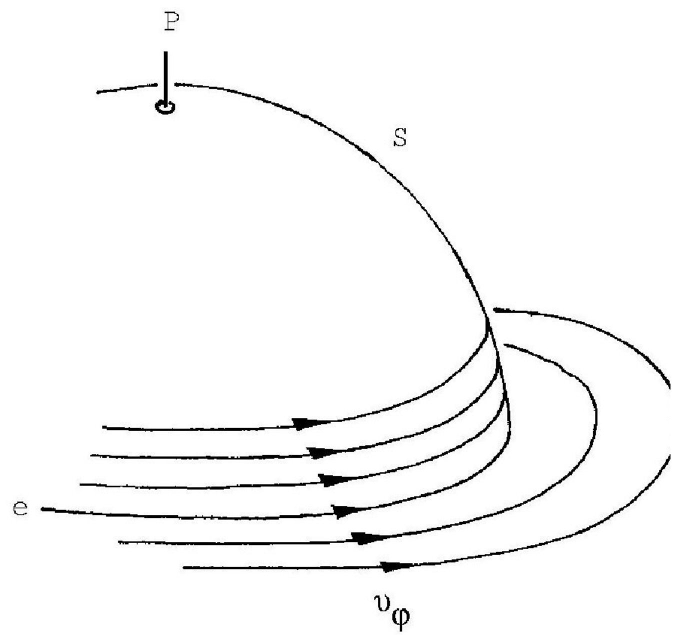

Inogamov & Sunyaev 1999

IXPE
Imaging X-Ray Polarimetry Explorer

Nonmagnetic NS: Cyg X-2

IXPE: PD=1.8±0.3% at PA=140±4 deg

OSO-8 (1976-1980):
PD=5.0±1.8% at PA=138±10 deg

Radio jet: PA=141 deg

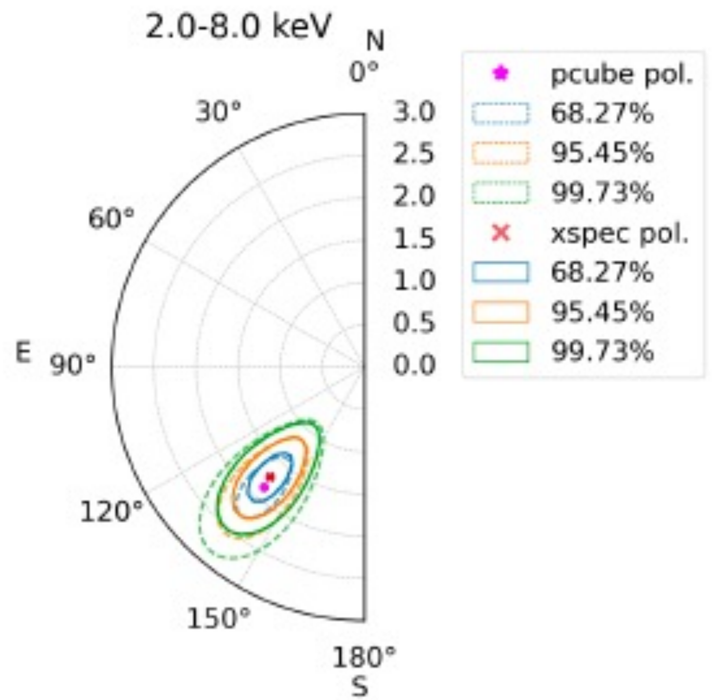

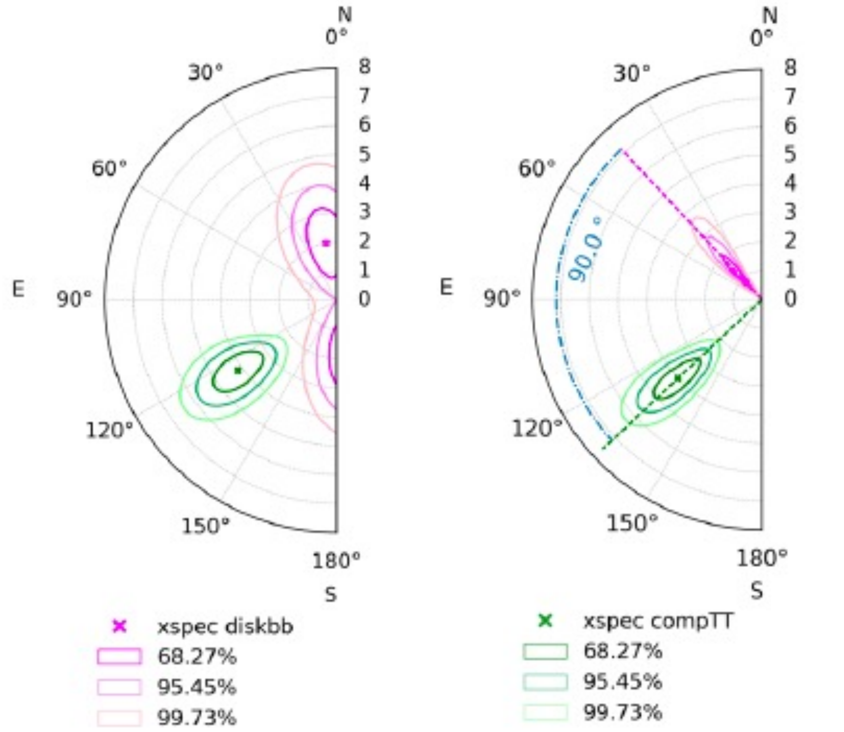

Figure 6. Contour plot of PD and PA in the 2–8 keV energy band obtained with XSPEC. The data have been fitted with two `polconst` models separately for the `diskbb` (pink colours) and `comptt` (green colours) components. *Left panel:* The PA of `diskbb` and `comptt` are left free. *Right panel:* The PA of `diskbb` was assumed to differ from the PA of `comptt` by 90°. Contour plots correspond to the 68.27%, 95.45% and 99.73% confidence levels, respectively.

Farinelli et al. 2023

Nonmagnetic NS: Cyg X-2

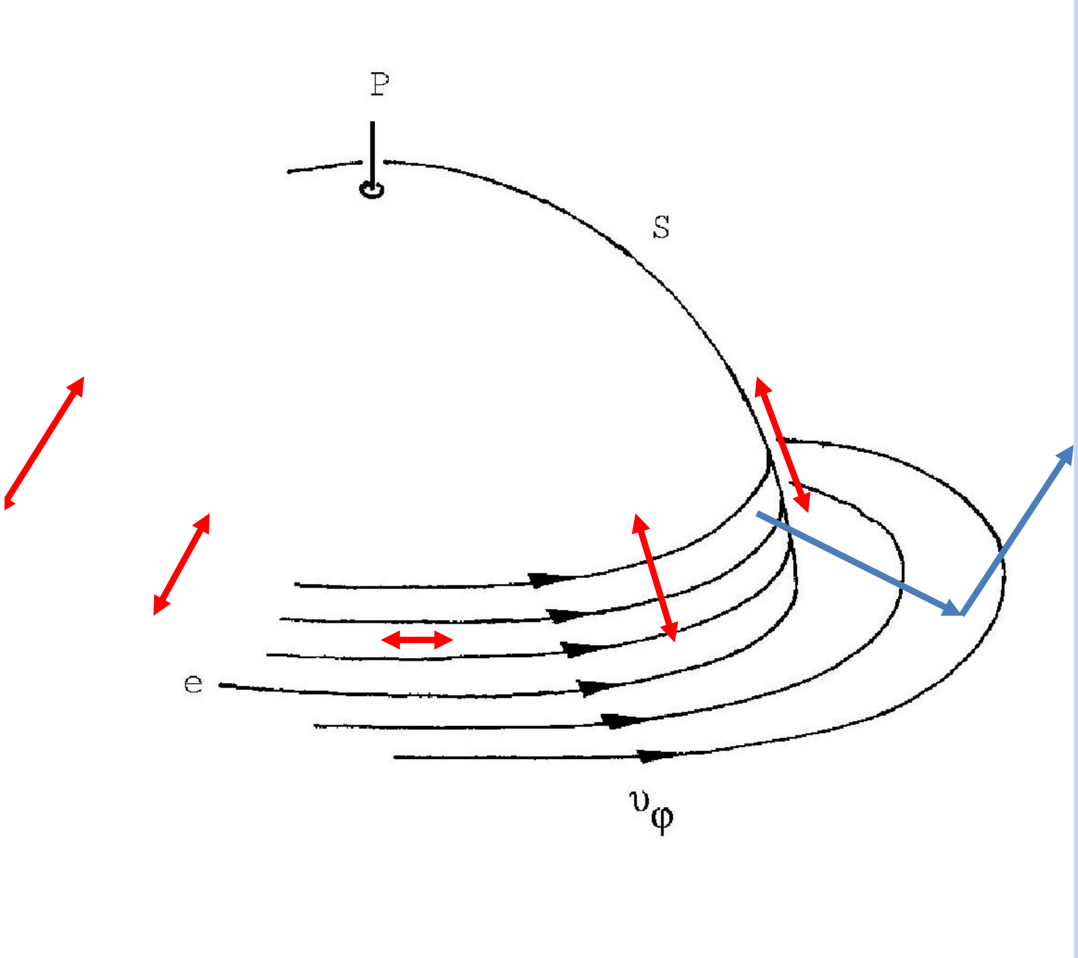

Where polarization is produced?

1. Spreading layer (Inogamov & Sunyaev 1999) ?
2. Reflection from the disk.
3. Scattering in a wind.

Polarization from the half-sphere is small. Maximum PD is 0.18% at i=60^o (Lapidus & Sunyaev 1985; but do not include relativistic effects).

Our new calculations show that it is difficult to get more than 1.5% even from a narrow belt (Bobrikova et al.).

Nonmagnetic NS: Cyg X-2

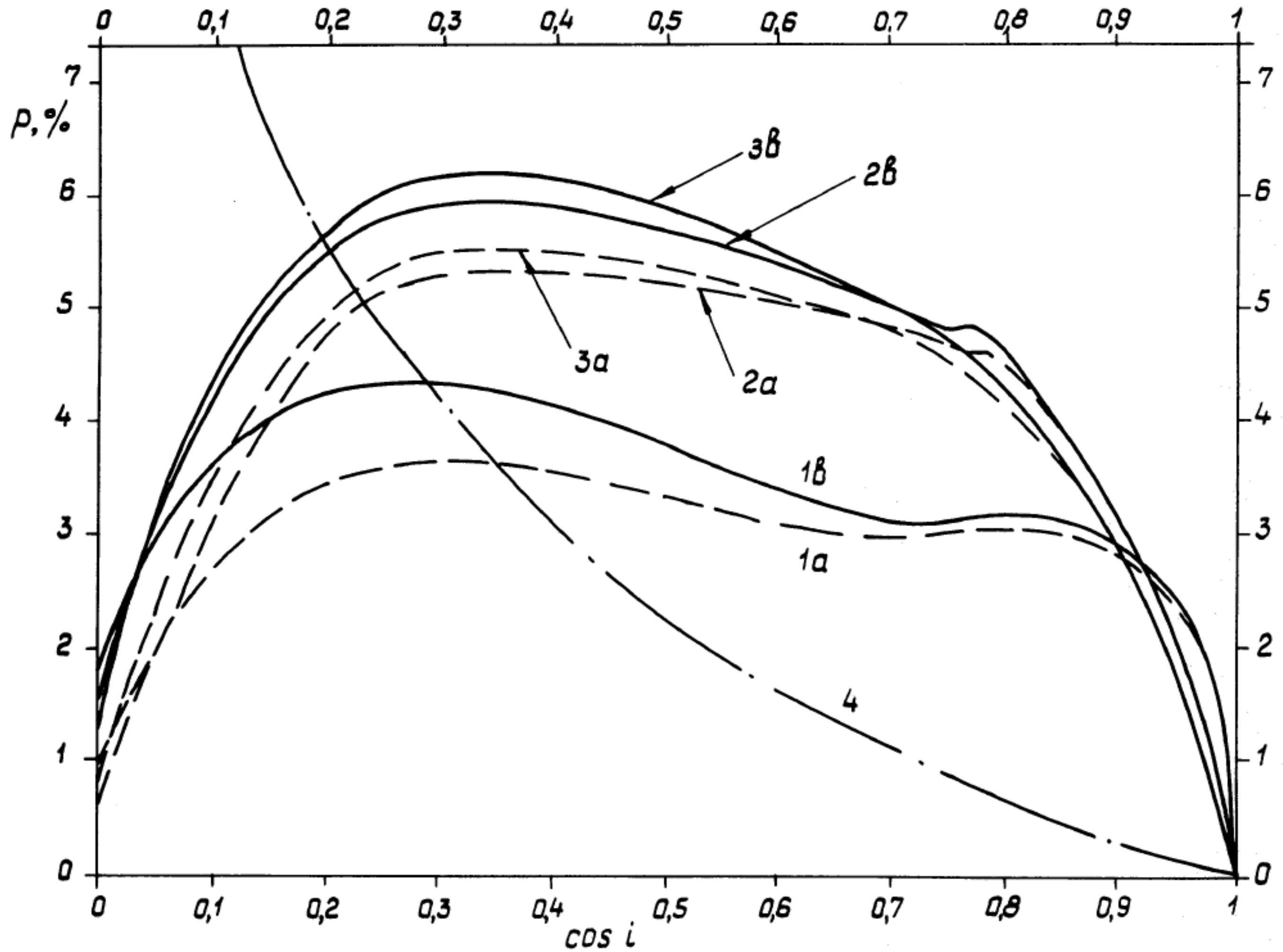

Figure 7. Degree of polarization of burster radiation between bursts. (1) H/R_s=0.05, (2) H/R_s=0.1, (3) H/R_s=0.2. Separately shown are (a) the polarization of disc radiation and (b) the polarization of radiation of the whole system 'disc+boundary layer'. The degree of polarization of radiation emitted by a semi-infinite electron scattering atmosphere (Chandrasekhar 1960) is also shown (4) for comparison.

2. Reflection from the accretion disk (Lapidus & Sunyaev 1985) ?

Up to 6% PD can be produced.

Models need to be updated to include relativistic effects.

Nonmagnetic NS: Cyg X-2

3. Thomson scattering in an equatorial wind (Sunyaev & Titarchuk 1985).

Chandrasekhar-Sobolev (optically thick electro-scattering dominated) case

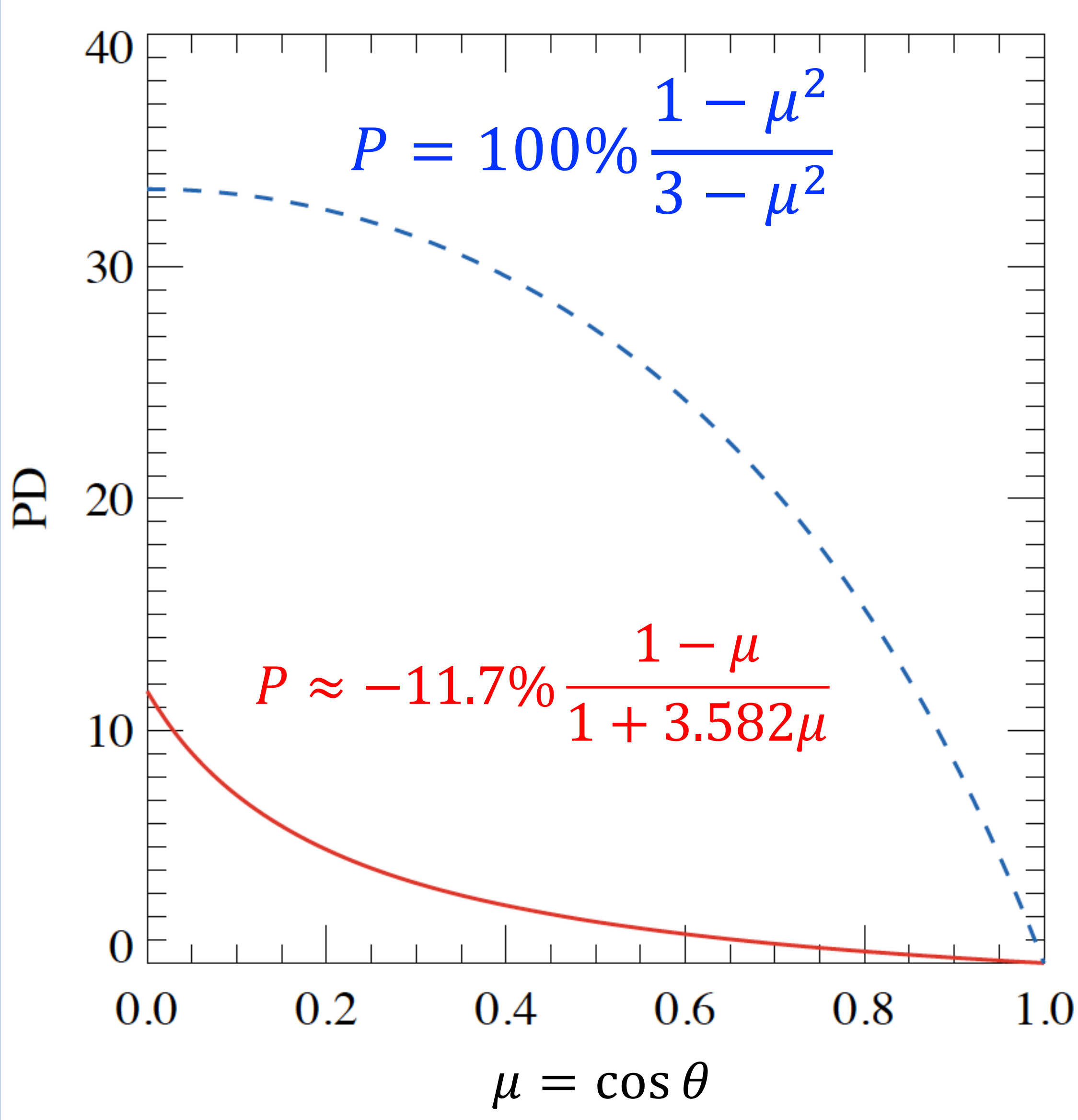

Nonmagnetic NS: Cir X-1

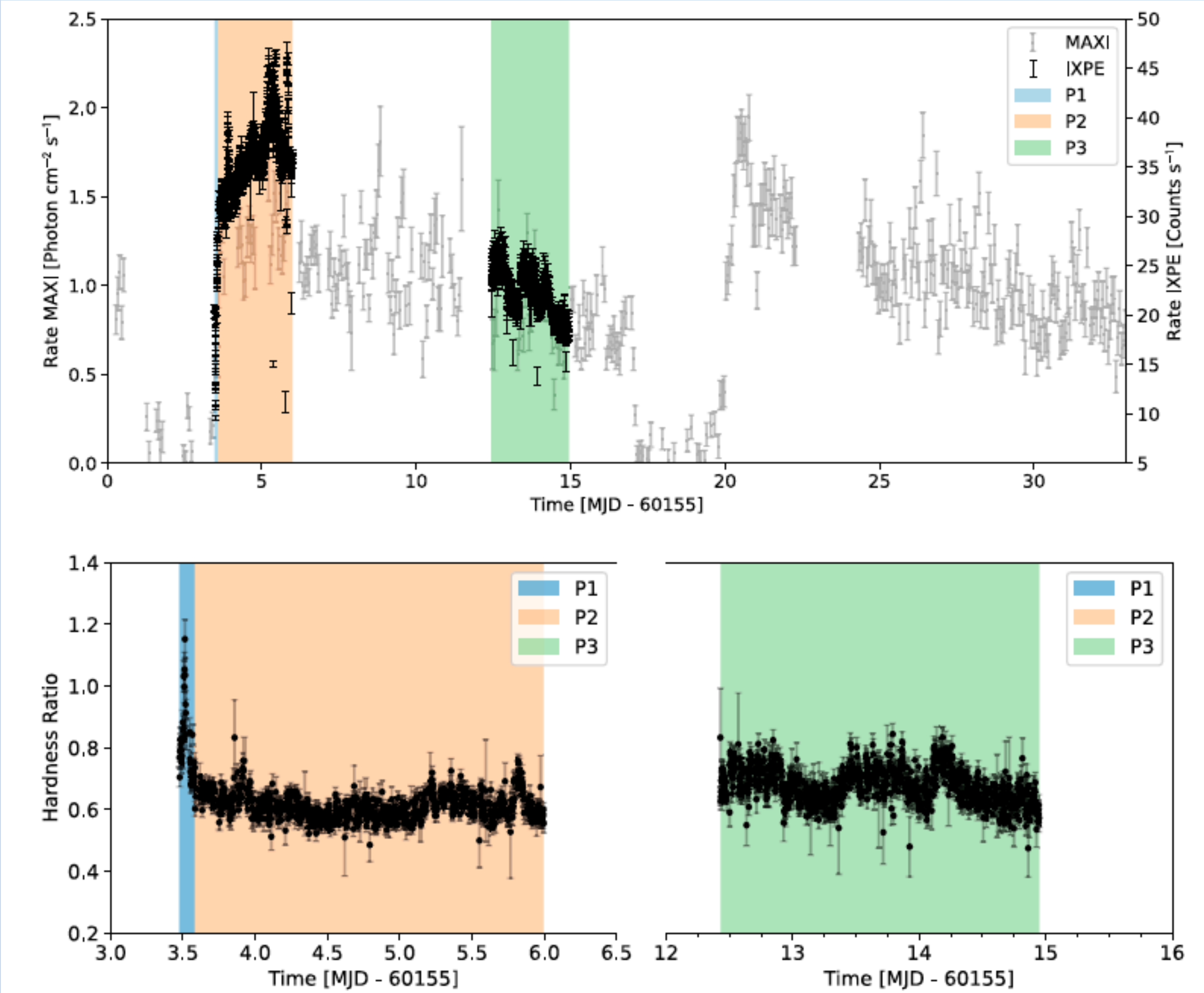

The youngest X-ray binary in the Galaxy, <5000 yr.

Orbital period of 16.6 d.

IXPE observed twice for about 130 ks each time.

Rankin et al. 2024

IXPE
Imaging X-Ray Polarimetry Explorer

Nonmagnetic NS: Cir X-1

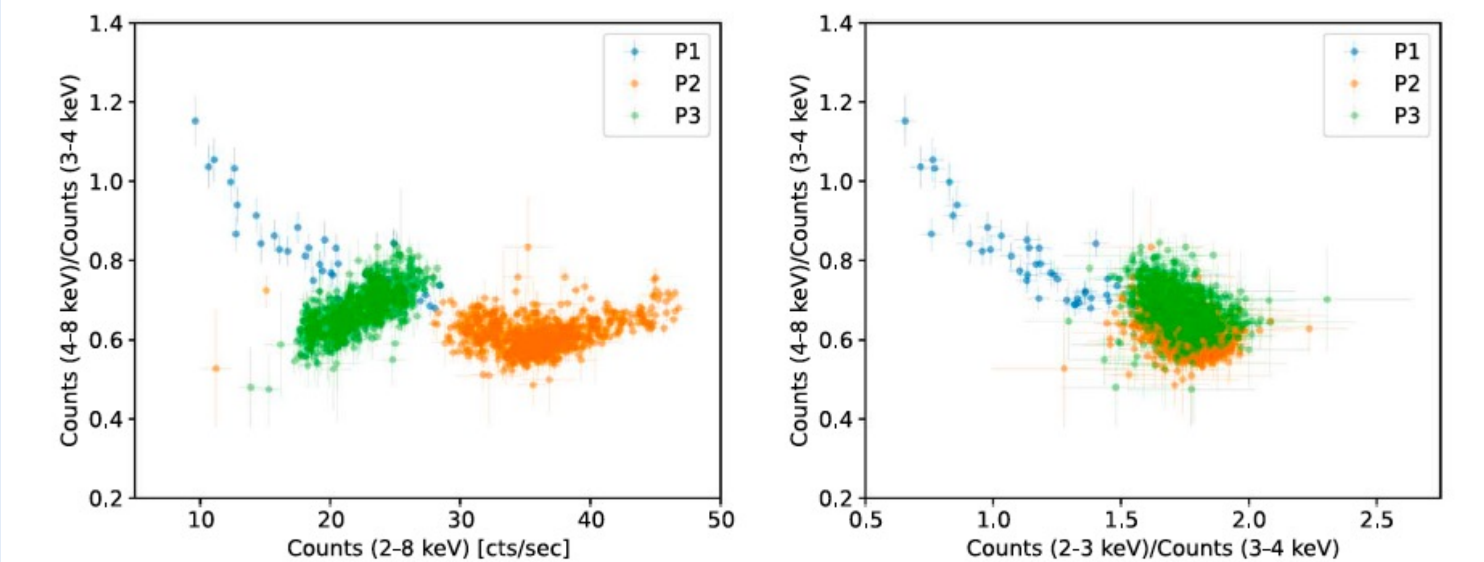

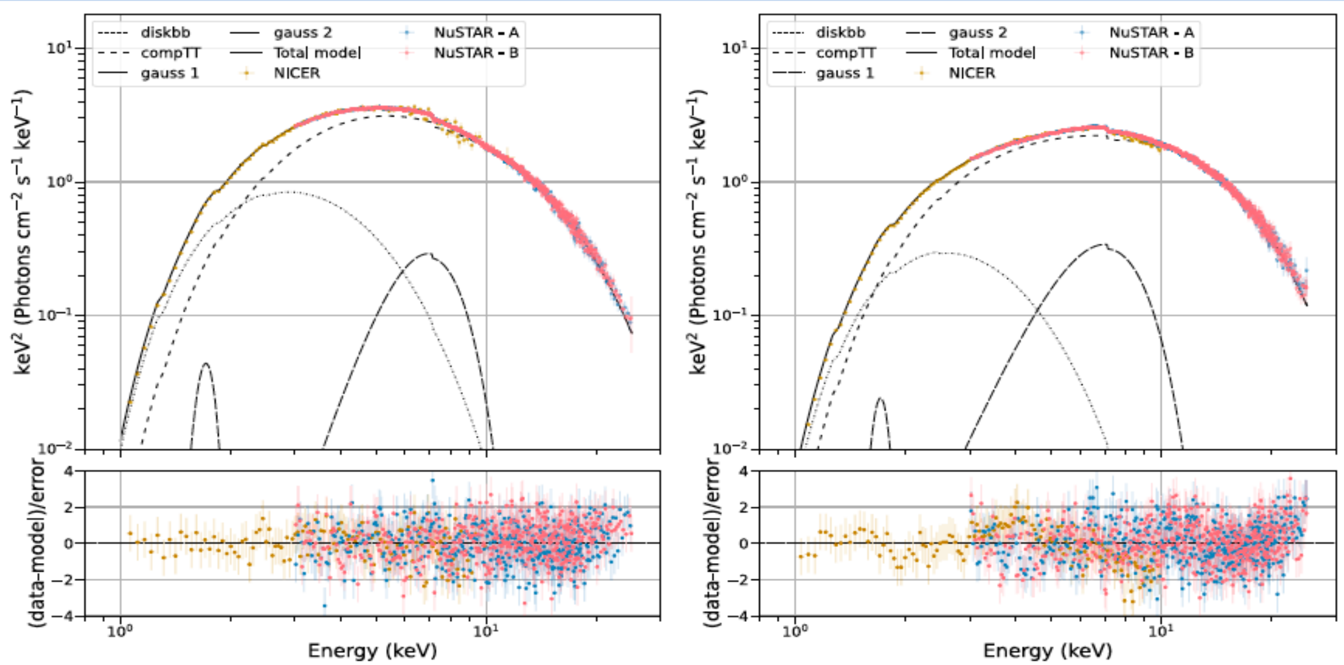

Rankin et al. 2024

Nonmagnetic NS: Cir X-1

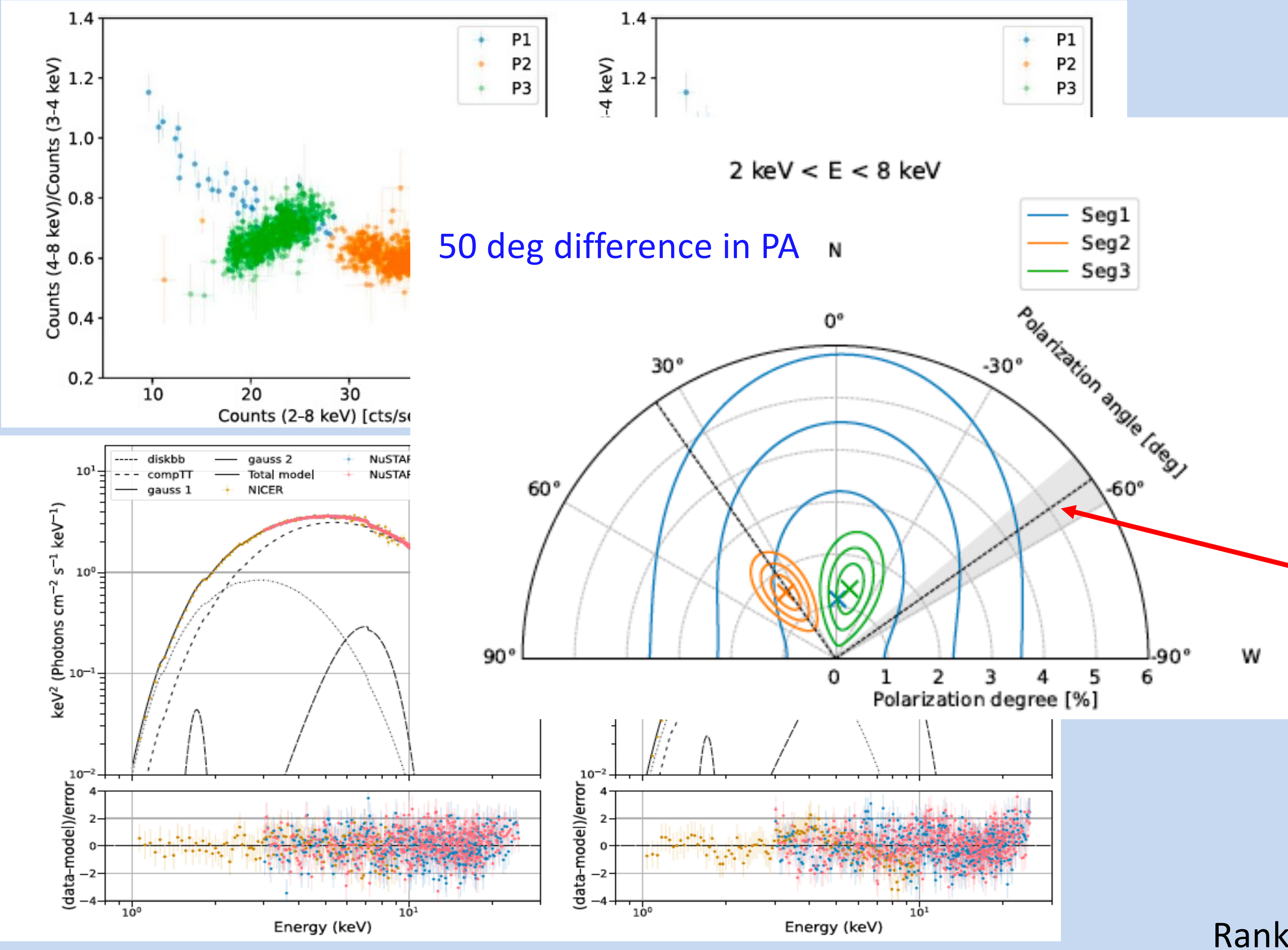

50 deg difference in PA

jet

Rankin et al. 2024

Nonmagnetic NS: Cir X-1

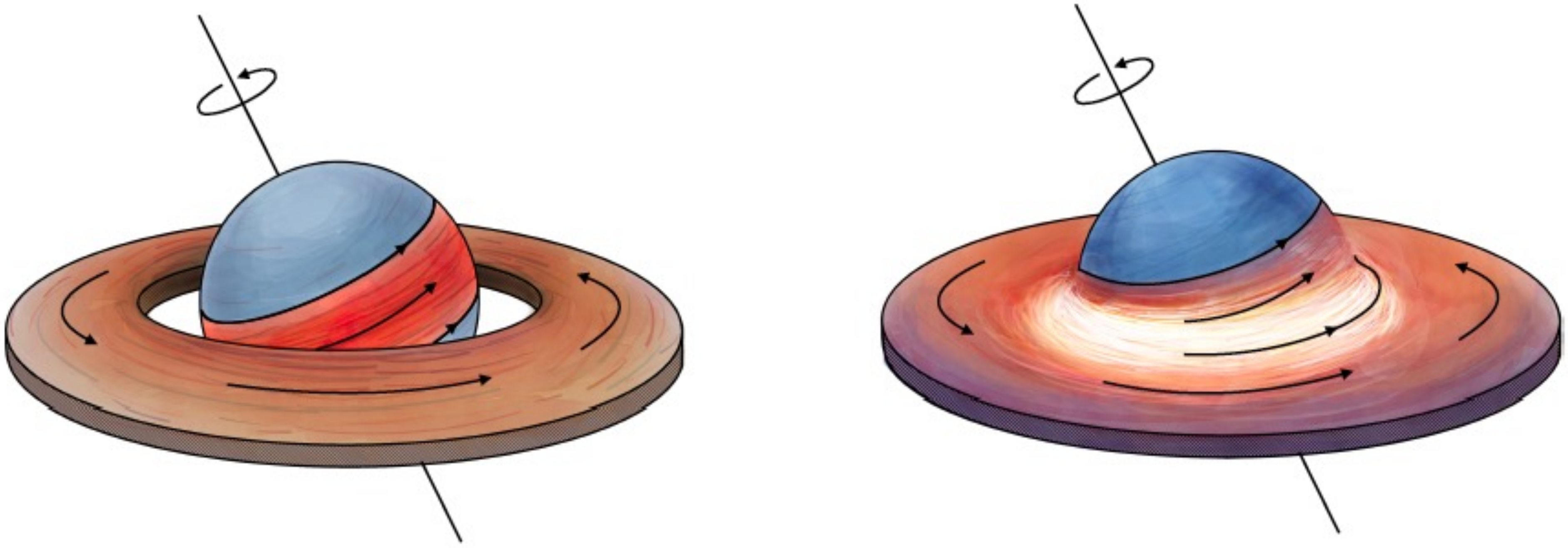

Evidence for misalignment of the neutron star spin from the orbital spin.

Rankin et al. 2024

Nonmagnetic NS: GX 13+1

- X-ray binary, dipper
- Inclination around 70 deg
- 24.5 day orbit
- Companion K5 III
- Observed by IXPE in October 2023

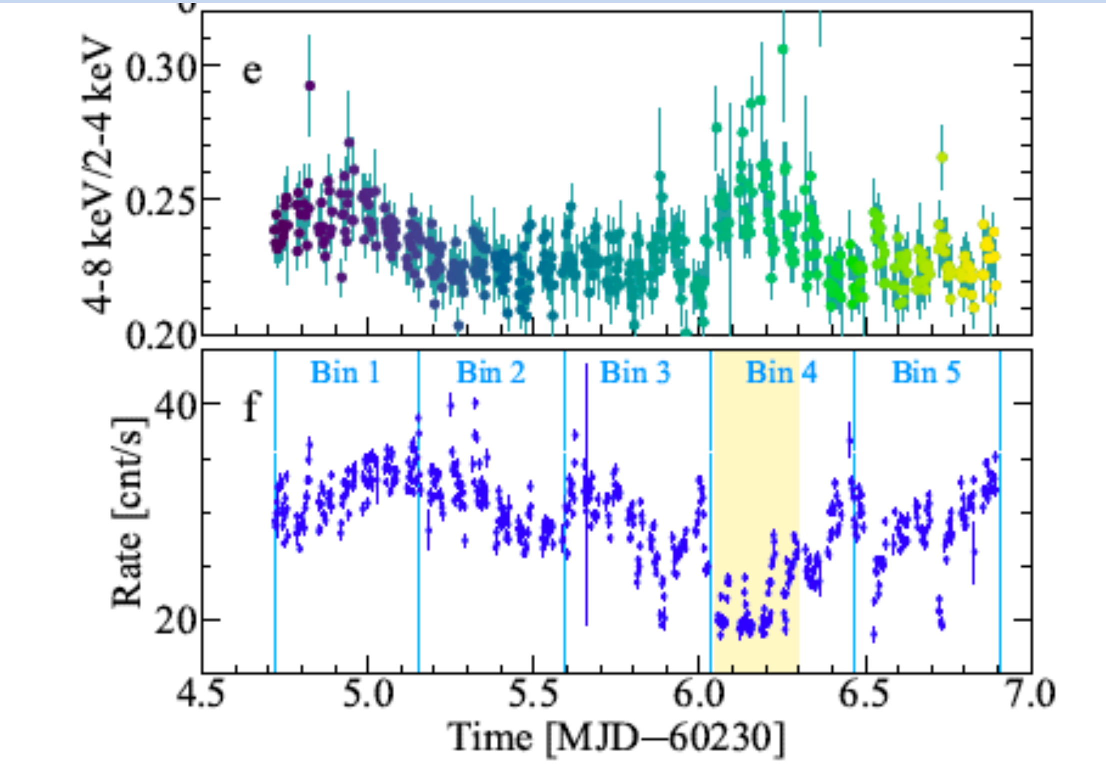

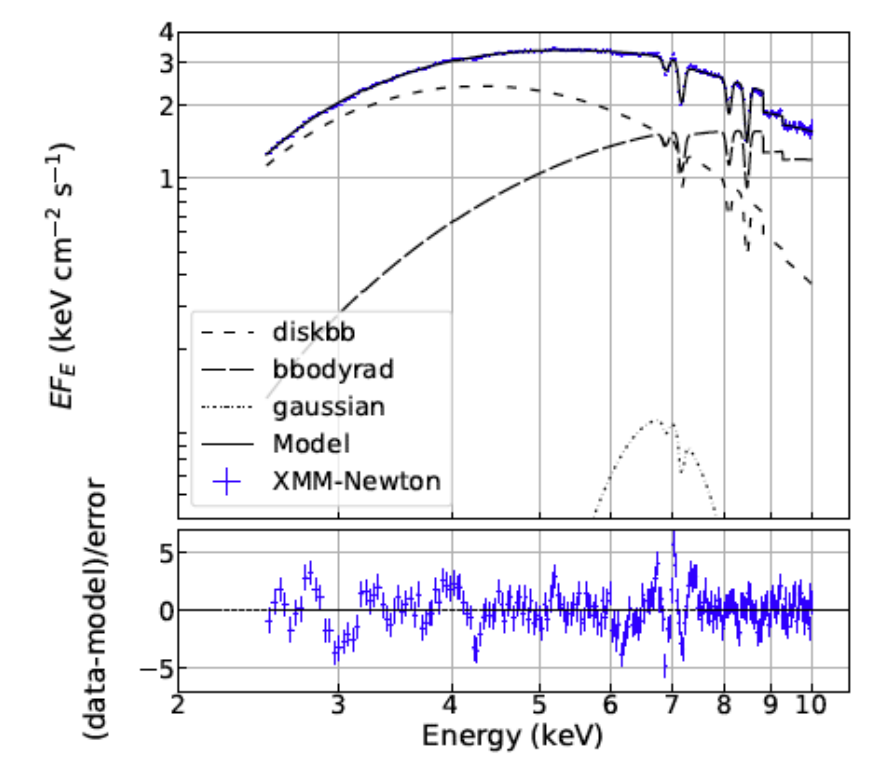

Bobrikova et al. 2024a

Nonmagnetic NS: GX 13+1

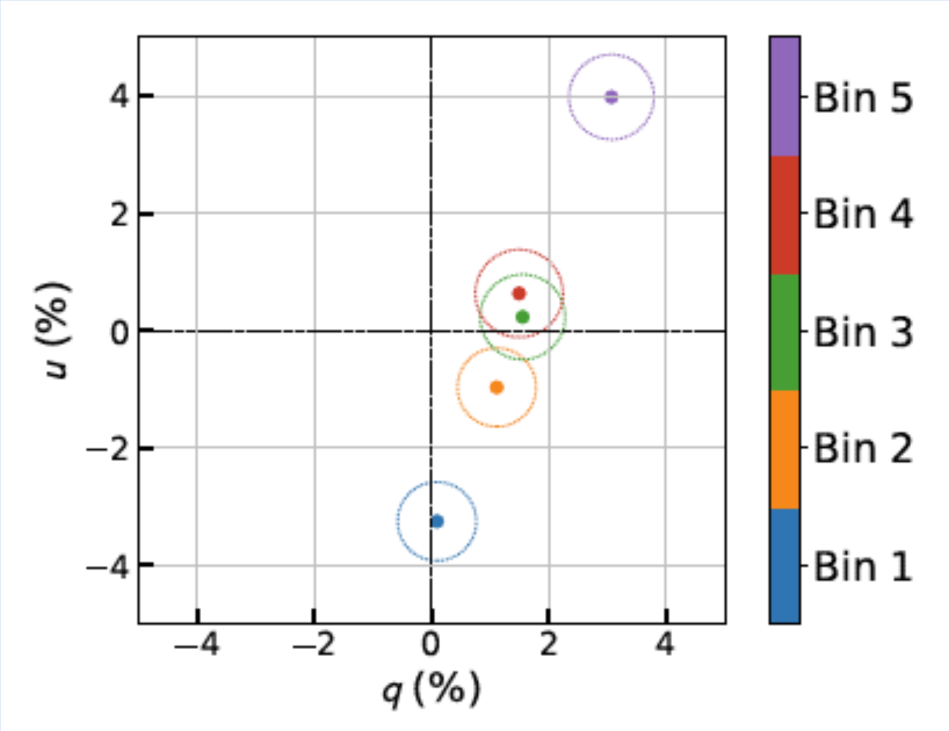

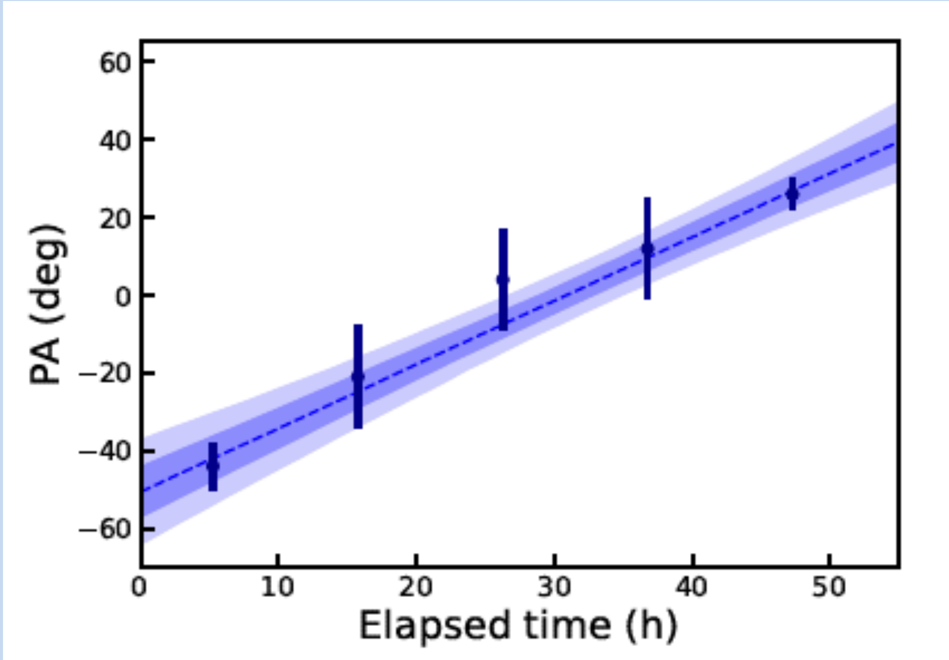

Rotation of the PA by 70 deg !

Bobrikova et al. 2024a

Nonmagnetic NS: GX 13+1

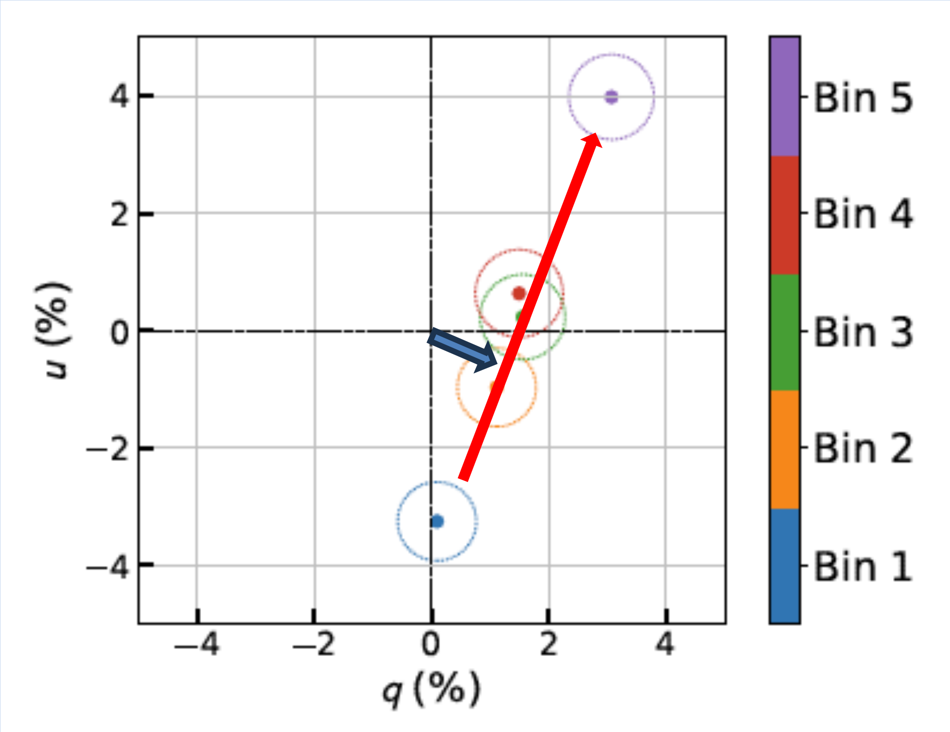

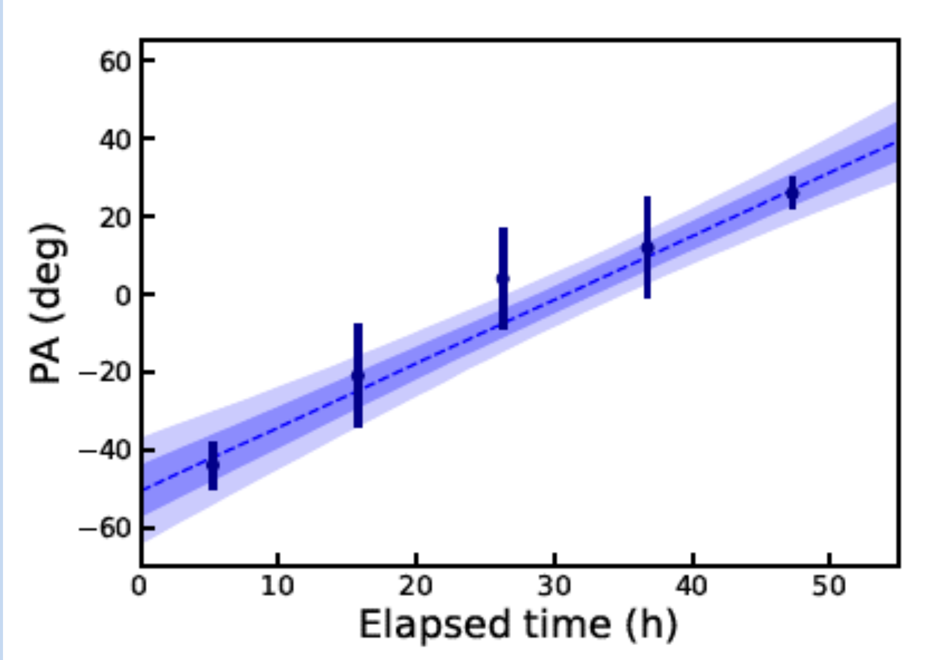

Rotation of the PA by 70 deg !

Evidence for two components?

Is the NS spin misaligned from the orbital one?

Or maybe strong azimuthal asymmetry of the disk wind?

Bobrikova et al. 2024a

Conclusion

- IXPE has opened a new window to the Universe.
- Observations of X-ray polarization has revolutionized our understanding of X-ray binaries.
- IXPE allows to measure geometry of emission region in accreting black holes and neutron stars.
  - X-ray pulsar geometry was uncovered. Precession of Her X-1 confirmed.
  - Additional polarized component was discovered in XRPs likely associated with the wind.
  - Found evidence of misalignment of nonmagnetic NS or strong anisotropy of the disk wind.